CATABOLISM OF STRUCTURALLY DIVERSE FRUCTANS BY BOVINE-ADAPTED BIFIDOBACTERIUM AND LACTOBACILLUS SPECIES IN PURE CULTURE AND EX VIVO RUMEN MICROBIAL COMMUNITIES

MARISSA KING
Bachelor of Science, University of Lethbridge, 2020

A thesis submitted
in partial fulfillment of the requirements for the degree of

MASTER OF SCIENCE

in

BIOCHEMISTRY

Department of Chemistry and Biochemistry
University of Lethbridge
LETHBRIDGE, ALBERTA, CANADA

CATABOLISM OF STRUCTURALLY DIVERSE FRUCTANS BY BOVINE-ADAPTED BIFIDOBACTERIUM AND LACTOBACILLUS SPECIES IN PURE CULTURE AND EX VIVO RUMEN MICROBIAL COMMUNITIES

MARISSA KING

Date of Defense: September 8th, 2022

Dr. D. Wade Abbott Dr. Trushar R. Patel Thesis Co-Supervisors	Research Scientist Assistant Professor	Ph.D. Ph.D.
Dr. Trevor Alexander Thesis Examination Committee Member	Research Scientist	Ph.D.
Dr. Anthony Russell Thesis Committee Member	Associate Professor	Ph.D.
Dr. Michael Gerken Chair, Thesis Examination Committee	Professor	Ph.D.

Dedication

This is dedicated to my parents, Richard and Shawna King for providing me with the means to explore my passion for research. Thank you for your love and support, and for always asking about my experiments even if you did not fully understand.

Abstract

Inulin and inulin-derived fructooligosaccharides (FOS) are well-known prebiotics for use in monogastric animals, but their potency in ruminants has not been determined. Additionally, structurally diverse fructans, such as graminan-type fructans purified from immature cereal crops may also possess prebiotic potential. As the composition of the rumen microbiome is closely associated with traits, such as: feed utilization, health, and waste production; prebiotics and probiotics are promising additives that can shift the microbial community towards a more productive state. In this thesis, the ability of bovine-adapted *Bifidobacterium* and *Lactobacillus* species to utilize FOS, inulin, levan, and graminans was assessed. Fluorescently labelled fructans and FISH were performed to directly visualize fructan interactions with *Bifidobacterium* and *Lactobacillus* species at the single-cell level. The prebiotic potential of inulin was compared between naïve or inulin-adapted microbial communities. This research provides new methods and benchmarks for evaluating fructans derived from diverse sources as prebiotic candidates in cattle.

Acknowledgements

Firstly, I would like to thank my supervisor, Dr. Wade Abbott for the tremendous amount of support and guidance he has provided throughout both my undergraduate and graduate degrees. I would also like to thank my co-supervisor Dr. Trushar Patel, and my committee members, Dr. Trevor Alexander and Dr. Tony Russell for their guidance and expertise. A special thank you to Leeann Klassen and Dr. Geta Reintjes for sharing their knowledge and expertise regarding the presented work on fluorescently labelled polysaccharide generation and visualization. Thank you to Dr. Greta Reintjes, Dr. Kristin Low and Jeffrey Tingley for their key roles in CAZomic analyses and SACCHARIS plotting using R Studio. Thank you to Dr. Xiaohui (Mike) Xing for sharing his vast knowledge on glycomics, and to Darrell Vedres for providing work towards the presented analytical chemistry work.

I would like to acknowledge Dr. Trevor Alexander's lab, including Dr. Long Jin and Dr. José de Jesús Ortiz Guluarte who were essential for the animal trial and the collection of rumen samples that gave rise to the work presented in chapter 3. I would also like to acknowledge the Beef Cattle Research Council (BCRC), who provided funding for this project.

Lastly, I would like to thank all other past and present members of Dr. Abbott's lab whom I have had the pleasure to work with: Dr. Darryl Jones, Dr. Jolene Garber, Dr. Julie Grondin, Dr. Carolyn Amundsen, Adam Smith, Stephanie Monteith, Marshall Smith, Jaclyn McMillan, Barinder Bajwa, Vanessa Mertens, and Nic Jujihara,

This work would not be possible without all of you.

Table of Contents

List of Tables

List of Figures

List of Abbreviations

AA	Auxiliary Activity
ABC	ATP-Binding Cassette
AUC	Area Under the Curve
B. boum	*Bifidobacterium boum* (ATCC 27917)
B. globosum	*Bifidobacterium psuedolongum* subsp. *globosum* (ATCC 25865)
BK	Barley Kernel
B. merycicum	*Bifidobacterium merycicum* (ATCC 49391)
B. ruminantium	*Bifidobacterium ruminantium* (ATCC 49390)
BS	Barley Stem
cfMRS	Carbohydrate-free De Man, Rogosa, and Sharpe
cfTPY	Carbohydrate-free Tripticase Phytone Yeast extract
CAZymes	Carbohydrate Active enZymes
CBM	Carbohydrate Binding Module
CE	Carbohydrate Esterase
CNBr	Cyanogen Bromide
CV	Column Volume
DAA	Days After Anthesis
DAPI	4', 6-diamidino-2-phenylindole
DP	Degree of Polymerization
FA	Formaldehyde
FACseq	Fluorescence Activated Cell sorting and sequencing
FCR	Feed Conversion Ratio
FITC	Fluorescein isothiocyanate
FISH	Fluorescence *In Situ* Hybridization
FLA	Fluoresceinamine
FLA-BK	Fluoresceinamine-Barley Kernel fructans
FLA-BS	Fluoresceinamine-Barley Stem fructans
FLA-inulin	Fluoresceinamine-inulin
FLA-levan	Fluoresceinamine-levan
FLA-PS	Fluorescently Labelled Polysaccharide
FLA-YM	Fluoresceinamine-yeast α-mannan
FOS	Fructooligosaccharide
GH	Glycoside Hydrolase
GI	Gastrointestinal
GT	Glycosyl Transferase
HPAEC-PAD	High-Performance Anion-Exchange Chromatography with Pulsed Amperometric Detection
L. ruminis	*Lactobacillus ruminis* (ATCC 27780)
L. vitulinus	*Lactobacillus vitulinus* (ATCC 27783)
LC-ESI-MS/MS	Liquid Chromatography ElectroSpray Ionization tandem Mass Spectrometry
MRS	De Man, Rogosa, and Sharpe
NMDS	Non-metric Multi-Dimensional Scaling
TPY	Tripticase Phytone Yeast extract
PBS	Phosphate Buffered Saline

PUL	Polysaccharide Utilization Locus
PL	Polysaccharide Lyase
RFI	Residual Feed Intake
SACCHARIS	Sequence Analysis and Clustering of CarboHydrate Active enzymes for Rapid Informed prediction of Specificity
SGBP	Surface Glycan Binding Protein
SPE	Solid Phase Extraction
SR-SIM	Super Resolution – Structured Illumination Microscopy
SWK	Spring Wheat Kernel
SWS	Spring Wheat Stem
VFA	Volatile Fatty Acid
WWK	Winter Wheat Kernel
WWS	Winter Wheat Stem
YM	Yeast α-mannan

Chapter 1

Literature Review

1.1 Sustainable beef production

The global human population is predicted to reach 9.8 billion by 2050 [1]. This increase will put additional pressure on the agricultural industry to provide crop and livestock derived food products. For beef producers in particular, a 1.2% increase in beef consumption is expected to occur every year until 2050 [2]. Additionally, these producers face public scrutiny about the environmental costs of beef production, such as the use of fresh water and cultivatable land [3], and waste generation, such as manure and enteric methane [3, 4]. Looking forward, the beef industry will focus on improving production efficiency to ensure future food security [5]. As such, research efforts funded by producer agencies, such as the Beef Cattle Research Council, are being directed towards improving the production efficiency of cattle and their feed [4].

Feed efficiency is the amount of valued product produced from the feed consumed. Traditionally, a feed conversion ratio (FCR) was used to measure feed efficiency, however use of this measurement does not account for the feed's nutritional value and is correlated with phenotypic and genetic growth measurements [6, 7]. Residual feed intake (RFI) has emerged as the current standard metric for evaluating feed efficiency in livestock. RFI was first defined by Koch *et al.* [8], as the difference between the observed and predicted feed intake that is required for growth and maintenance. A regression equation involving the animal's average daily gain and metabolic body weight is used to calculate RFI, where a low RFI value indicates that the animal is more efficient, consuming less feed than predicted while maintaining its production level [9].

Recently, Paz *et al.* [10] discovered that ~20% of variation within the feed efficiency and production traits of beef cattle (*i.e.,* average daily gain, average daily feed intake, and feed to gain ratio) were explained by compositional alterations in the rumen microbiome. Whilst many environmental, therapeutic, or intrinsic factors including host genetics and antimicrobials, play a role in influencing the microbial community [11, 12], diet was determined to be the main factor determining the relative abundance and composition of the rumen microbiome [13]. Considering the host-microbiota relationship and the effect diet has on the rumen microbiome, it may not be surprising that a wide range of dietary additives, such as prebiotics, probiotics, and essential oils, have been used to manipulate the rumen microbiome towards a more productive state [7, 14].

1.2 The rumen microbiome

Ruminants, such as Bovinae (*e.g.,* cattle, bison) and Caprinae (*e.g.,* sheep, goats), have evolved a specialized foregut that consists of four compartments: the rumen, reticulum, omasum, and abomasum. At birth, the ruminant digestive system is not fully functional, rather it develops over the weaning period as the calf transitions from milk to solid food [15]. Microbial colonization within the developing rumen begins as early as the first day of life [16], where milk oligosaccharides and glycoconjugates present in colostrum and milk promote the proliferation of beneficial Bifidobacteria and Lactobacilli [17, 18]. The abundance of these genera are known to decrease during the weaning period and were no longer detectable at nine weeks [19].

Following the transition to feed, a fully developed rumen houses a complex and dynamic microbial ecosystem consisting of anaerobic bacteria, protozoa, anaerobic fungi, methanogenic archaea, and phages; this community facilitates the digestion of feed prior

to it entering the abomasum [13, 20]. Henderson *et al.* [13] discovered a core rumen microbiome consisting of four dominant phyla: Bacteroidetes, Firmicutes, Proteobacteria, and Fibrobacter. Bacterial species belonging to Bacteroidetes (*e.g., Bacteroides thetaiotaomicron*), have been shown to be prolific at metabolising polysaccharides and possess polysaccharide utilization loci (PULs) within their genomes [21, 22]. PULs typically encode at least one transport system comprised of a surface glycan-binding protein (SusD) and TonB-dependent transporter (SusC), Carbohydrate-Active enZymes (CAZymes), and carbohydrate responsive transcriptional regulators [21]. Notably, the genes within a PUL are colocalized and coregulated. In contrast, there has been speculation whether Gram-positive species, such as those belonging to the Firmicutes (*e.g.*, *Eubacterium rectale*), and Actinobacteria (*e.g., Bifidobacterium bifidum*) phyla, contain PULs [23]. While these "Gram-positive PULs" lack the SusD and sensor/regulator type genes found within the PULs of Bacteroidetes, they possess a carbohydrate transport system (*e.g.,* ATP-binding cassette (ABC)), a transcriptional regulator (*e.g.,* LacI-like), and a minimum of one CAZyme [23, 24]. Additionally, extracellular solute binding proteins may be involved in substrate recognition and binding at the cell surface [23]. While the vast diversity of PULs and their associated CAZymes that are found within the rumen microbiome can be routinely identified with genetics (*e.g.,* shotgun whole genome metagenomics sequencing) and established bioinformatics pipelines [25], deciphering the chemical transformations of polysaccharides that occur during digestion is not as straight-forward. For instance, cross-feeding, or syntrophy, can occur amongst different microbial members of the rumen microbiome during polysaccharide metabolism, generating trophic-like levels of digestion [26].

1.3 Polysaccharides

Complex carbohydrates, in the form of oligosaccharides and polysaccharides, can be composed of various monosaccharide subunits connected by glycosidic linkages, generating a tremendous amount of structural diversity [27-29]. Within plant cells, different complex carbohydrates function as storage or structural polysaccharides. In the plant cell wall, cellulose, hemicellulose (*e.g.,* xyloglucan, mannan), and pectin (*e.g.,* homogalacturonan, rhamnogalacturonan II) polysaccharides provide the cell with mechanical integrity, whereas starch and fructans serve as storage polysaccharides, and are relatively simpler in their structure [29].

1.4 Fructans

1.4.1 Fructan polysaccharides

Fructans are fructose-based oligo- and polysaccharides in plants, fungi, algae, and bacteria. While fructans found in certain bacterial genera, such as *Erwinia* and *Pseudomonas*, have been found to exceed a degree of polymerization (DP) of 100 000; plant fructans are considerably smaller, having an average DP of 30 – 60 and a maximal recorded length of 200 [30]. Although small, plant fructans exhibit much more variation within their bond composition and glucose content, giving rise to five main classes of fructans that differ in their structural diversity: inulin, levan/phlein, graminan, neo-inulin, and neo-levan [31-35]. The most well-known type of fructan is inulin, a β-2,1 linked fructan composed of one terminal glucose residue and 3-60 fructose residues (Figure 1.1A). Inulin and its smaller fructooligosaccharides (FOS; DP 3 – 10) are found in *Asterales* plants, including chicory and Jerusalem artichoke [32]. Linear fructans containing β-2,6 linkages with a terminal glucose (Figure 1.1B) are known as levan. Previously, phlein was used to describe levan found in plants such as grasses from the

Poales order [32, 36], whereas levan was solely used to describe β-2,6 linked fructans synthesized by bacteria. Graminan-type fructans contain both β-2,1 and β-2,6 linkages giving rise to a branched polymer (Figure 1.1C), and are found within cereal crops, such as wheat (*Triticum aestivum* L.) and barley (*Hordeum vulgare* L.) [37-39]. Lastly, neo-inulin and neo-levan, collectively termed neoseries fructans, contain an internal glucosyl residue with either predominate β-2,1 or β-2,6 linkages, respectively [34, 38]. While neo-levans can also be found within the Poales order, neo-inulins are specifically found within Liliaceae and Asparagaceae families [40].

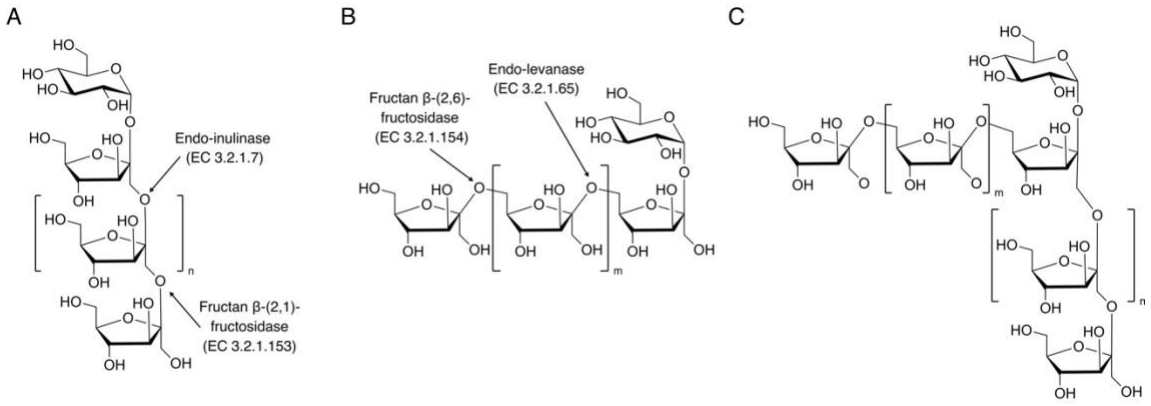

Figure 1.1: Structural variation seen in different types of fructans. (A) inulin, **(B)** levan, and **(C)** graminan.

1.4.2 Fructan-containing cereal crops

For most cereal crops, fructan serves as a reserve carbohydrate during the plant's immature growth phase before starch accumulation begins. When fructan is present, it has been shown to act as an osmoregulator protecting and regulating stress tolerance during harsh growing conditions, such as drought, extreme cold, and salinization [41-45].

Fructan metabolism within wheat has been well studied. Fructans are initially synthesized from sucrose in the vacuoles of vegetative tissue cells. These are small DP fructans and are stored in the vacuoles until anthesis occurs. After anthesis, stored fructan is hydrolyzed into sucrose and fructose where they are transported through phloem between vegetative tissues and developing kernels [42, 46]. In developing wheat kernels, the fructan concentration is known to change throughout three stages of kernel development, where fructan accumulation predominantly occurs within the first stage, cell division and expansion which lasts ~14 days after anthesis (DAA) [35, 38].

For mature cereal crops, it has been reported that rye contains the highest level of fructan ranging from 3.6 – 6.6% of the dry matter, whereas wheat and barley have been reported to contain lower levels at 0.7 – 2.9% and 0.9 – 4.2%, respectively [47, 48]. In contrast, the fructan concentration in immature kernels of wheat, rye, triticale, and barley, has been reported to range between 23.7 – 39.0% [49]. For individual wheat kernels, fructan content reaches its maximum concentration at 16 DAA, amounting to 2.5 ± 0.3 mg fructan/kernel, with an average DP of 7.3 ± 0.4 [38]. Fructans within these immature cereal crops have been found to be predominantly graminan, yet some neoseries fructans have also been reported [38, 50]. For beef producers, one promising alternative to purchasing industry-produced inulin and FOS prebiotics, is the utilization of on-farm,

immature crop residues that naturally contain high levels of fructans. This may include crops that were damaged by hail, severe drought, or shortened growing seasons. In this manner, damaged or immature cereal crops may represent a value-added source of prebiotics for ruminants [51, 52]. The role of prebiotics in rumen function is described in Section 1.6.

1.5 Carbohydrate-active enzymes

Ruminants rely on the digestive capabilities of the rumen microbiome. The remarkable carbohydrate utilization capacity of the rumen is the result of a vast CAZyme collection, specific for the depolymerization of diverse polysaccharides present within the feed. CAZymes are classified into five classes that catalyze the biosynthesis, breakdown, or modification of carbohydrates and glycoconjugates: glycosyltransferases (GTs), glycoside hydrolases (GHs), carbohydrate esterases (CEs), polysaccharide lyases (PLs), and auxiliary activities (AAs) [53]. GTs are responsible for catalyzing the formation of glycosidic bonds. AAs are enzymes with redox activities. CEs carry out the hydrolysis of carbohydrate esters. PLs use β-elimination to cleave polysaccharides containing uronic-acid groups. The largest CAZyme family is the GHs, which are responsible for the hydrolysis of glycosidic linkages.

Hydrolysis of a glycosidic linkage is carried out by two amino acid residues, where a general acid (*e.g.*, glutamic acid) acts as the proton donor and the second residue (*e.g.*, aspartic acid) is the nucleophile/base. Currently, there are 173 sequence related GH families [54]; where each family has a conserved fold, catalytic residues, and mechanism. However, the substrate specificity within a GH family can vary significantly, and in some cases, families are further classified into subfamilies [53, 55]. Families exhibiting

different specificities are referred to as polyspecific, and individual members may possess functions that have yet to be characterized. Use of *in silico* tools, such as SACCHARIS (Sequence Analysis and Clustering of CarboHydrate Active enzymes for Rapid Informed prediction of Specificity) [56], dbCAN2 [57, 58], CUPP [59], and eCAMI [60] can help streamline accurate predictions of uncharacterized CAZyme functions using sequence data.

While CAZymes are classified into families based on the enzyme's structural features, certain families seem to be reflective of substrate structure as well. For instance, members belonging to the GH32 family are known to cleave the β-2,6 and β-2,1 linkages present within different fructan polysaccharides [61]. Depending on their mode of action, GH32s are known to be β-fructofuranosidases, endo- and exo-acting inulinases and levanases, or non-specific fructan β-fructosidases. Interestingly, several different fructosyltransferases (EC 2.4.1.-, 2.4.1.10, 2.4.1.100, 2.4.1.243, 2.4.1.99) are also a part of this family, suggesting a role in fructan biosynthesis [54]. Other enzymes acting upon fructans are found within the GH68 family, including inulosucrases and levansucrases, where sucrose is the preferential donor substrate [54]. Both families share the common structural feature of a 5-bladed β-propeller domain and are classified into the clan GH-J [62].

1.6 Prebiotics, probiotics, and synbiotics

A prebiotic is "a substrate that is selectively utilized by host microorganisms conferring a health benefit" [63]. When a prebiotic (*e.g.,* oligo- or polysaccharide) is consumed in sufficient amounts, it may selectively stimulate the proliferation and/or activity of beneficial microbes present within the gut, such as Bifidobacteria and

Lactobacilli [64]. A majority of commercialized prebiotics are carbohydrates, such as galactooligosaccharides, maltooligosaccharides, lactulose, and FOS [65], and their effects have been studied in humans and monogastric animals, such as calves, swine, and poultry [66, 67]. Previous studies evaluating the effects of FOS on calf growth have been shown to be variable, where two studies demonstrated improved feed efficiency and growth of calves [68, 69] or no difference [70, 71]. In terms of ruminants, very few studies investigating the potential prebiotic effect of inulin have been conducted. One study determined that 2% inulin supplementation into the low concentrate diet of finishing beef steers increased volatile fatty acid (VFA) production and final body weight, with a decreased FCR for an overall improved growth performance [72].

Unfortunately, there is much less information available regarding the prebiotic potential of other fructans (*e.g.,* graminan, neoseries), as they are not yet commercialized. The health effects of immature wheat grains have started to be evaluated in human and mice trials [73, 74], however the results of these studies are confounding as the wheat grains used in these studies contain other dietary fibers that may account for some of the results seen, such as increased satiety. Moving forward, studies using purified fructans from immature cereal crops are needed to determine their prebiotic potential.

Probiotics consist of "live microorganisms that, when administered in adequate amounts, confer a health benefit on the host" [64]. The inclusion of probiotics may enhance the host's gastrointestinal (GI) health by stimulating the development of a healthy gut microbiota, preventing pathogen colonization, increasing digestion efficiency, managing pH, improving mucosal immunity, and increasing VFA production [75]. For ruminants, the administration of probiotics has been examined at different life stages and with different microbial species. For instance, *Bacillus* and *Lactobacillus* species have

been administered to pre-ruminant calves to promote pathogen exclusion [19], whereas *Saccharomyces cerevisiae* and *Lactobacillus* species have been applied to adult ruminants to improve fiber digestion and limit acidosis that can commonly occur with high concentrate diets, respectively [76, 77]. Additionally, members belonging to the *Bifidobacterium* genus have gained popularity in both human and animal studies for their probiotic effects by providing a stable, nutrient-rich gut environment [78].

A synbiotic is defined as "a mixture comprising live microorganisms and substrate(s) selectively utilized by host microorganisms that confers a health benefit on the host" [79]. This combination can be classified as complementary or synergistic. A complementary synbiotic contains recognized prebiotics and probiotics, versus a synergistic synbiotic that contains a substrate that is consumed by the co-administered live microorganism to enhance its health benefits within the host [79]. For instance, the application of Bifidobacteria and/or Lactobacilli with FOS in synbiotic products for monogastric animals has recently gained attention over the last few years, as products like PoultryStar® (ME BIOMIN GmbH) are now available [67]. This synergistic synbiotic formulation is based on the well-studied effect FOS has on stimulating the growth and activity of Bifidobacteria and Lactobacilli [80, 81].

1.7 Fluorescently labelled polysaccharides

Fluorescently labelled polysaccharides (FLA-PS) were first developed by Glabe *et al.* [82]. In this reaction, the hydroxyl group of monosaccharide residues within a polysaccharide are stochastically activated using cyanogen bromide (CNBr) and conjugated with fluoresceinamine (FLA; Figure 1.2A), a fluorescent dye, through its amine group (Figure 1.2B). Initially, Arnosti used FLA-laminarin and FLA-pullulan as

investigative tools to measure the hydrolysis rates of marine bacterial enzymes [83]. Since then, the hypothesis that FLA-PS were "too bulky" for cellular importation was disproven by Reintjes *et al*. [84], using super resolution structured illumination microscopy (SR-SIM) to visualize FLA-PS in the periplasm. The development of FLA-PS has ushered a powerful, "direct" method to visualize polysaccharide utilization by intestinal bacteria [84, 85]. This method has been used to investigate the prebiotic effects of yeast α-mannan (YM) on bacterial members in the rumen microbiome [86]. By coupling FLA-PS to other ecological methods, such as fluorescence *in situ* hybridization (FISH) or fluorescence activated cell sorting and sequencing (FACSeq), metabolically active bacteria can be identified, sorted, and characterized based upon their metabolic potential.

Recently, one dominant phylum from the core rumen microbiome has been identified using the combination of FLA-PS and FISH. In 2021, Klassen and Reintjes *et al.* [86], applied fluorescently labelled YM (FLA-YM) to rumen samples to directly visualize the metabolism of YM by rumen bacteria at the single cell level. 6.1 ± 0.5% of cells showed uptake of YM, where *Bacteroides* members identified using FISH accounted for ~3% of these cells. The use of this technique in complex communities, such as the rumen microbiome, suggests it can be extended to other substrates and rumen bacteria to evaluate prebiotic candidates. So far, this combined FLA-PS/FISH method has been limited to Gram-negative bacteria and *Planctomycetes* spp., which possess a periplasm or paryphoplasm, respectively. Its potential for studying uptake by Gram-positive species, such as *Bifidobacterium* spp. and *Lactobacillus* spp., has yet to be determined.

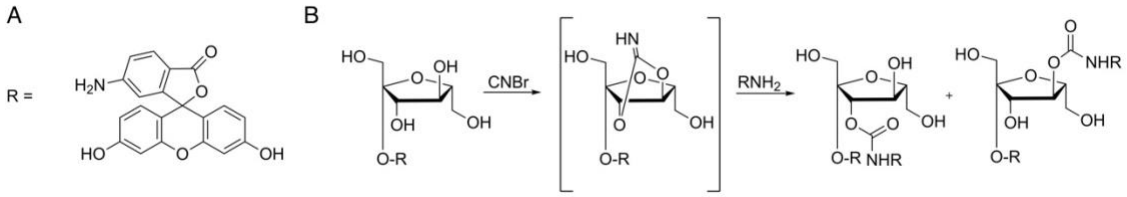

Figure 1.2: Fluorescent derivatization of fructan. (A) structure of the fluorophore, fluoresceinamine (FLA), **(B)** proposed chemical mechanism of FLA conjugation to a fructose residue within fructan.

1.8 Hypothesis

While inulin is an accepted prebiotic for humans and monogastric animals, it has yet to be adopted for use in cattle. Additionally, more complex fructans (*i.e.,* branching, mixed β-2,1 and β-2,6 glycosidic linkages) present in immature cereal crops, are expected to have prebiotic qualities as well, and may represent an inexpensive, on-farm alternative to commercial prebiotics. The growth of rumen bacteria on inulin and immature cereal crop fructans would indicate that these species encode the requisite CAZymes (*i.e.*, GH32s) required for fructan utilization. Bacteria with the potential to metabolize fructans can be studied using the FLA-PS method by directly visualizing uptake of fructans.

This thesis will test the hypothesis: Bovine-adapted *Bifidobacterium* and *Lactobacillus* species encode the appropriate CAZymes required for the degradation of inulin and mixed-linkage fructans derived from immature cereal crops. Whereby, supplementation with different fructan types will result in distinct responses and metabolic outputs that can be correlated with the structural variations of fructans.

1.9 Objectives

1. Isolate and characterize the structure of fructans found within the kernel and stem fractions of immature winter wheat, spring wheat, and barley collected seven days after anthesis (7 DAA), by HPAEC-PAD and LC-ESI-MS/MS.
2. Characterize the anaerobic growth of bovine-adapted *B. boum, B. merycicum, B. ruminantium, B. globosum, L.* ruminis, and *L. vitulinus* when FOS, inulin, levan, and fructans purified from the kernel and stem fractions of immature winter wheat, spring wheat, and barley (7 DAA) are incorporated as the sole carbohydrate source.

3. Evaluate the prebiotic effect of inulin in complex communities using artificial rumen batch cultures by measuring the production of VFAs, ammonia, gas, and 16S metagenomics sequencing.

4. Identify genes encoding putative CAZymes for fructan digestion from whole genome sequences of rumen bacterial species using the bioinformatics tools dbCAN2 and SACCHARIS.

5. Conjugate fluoresceinamine (FLA) to fructan polysaccharides to generate FLA-inulin, FLA-levan, FLA-BK, and FLA-BS, and visualize bacterial uptake of the fluorescent conjugates using epi-fluorescence microscopy and SR-SIM in pure cultures of *B. boum, B. merycicum, B. ruminantium, B. globosum, L.* ruminis, and *L. vitulinus* and rumen samples *ex vivo* in combination with Bif228 and Lac722 FISH probes.

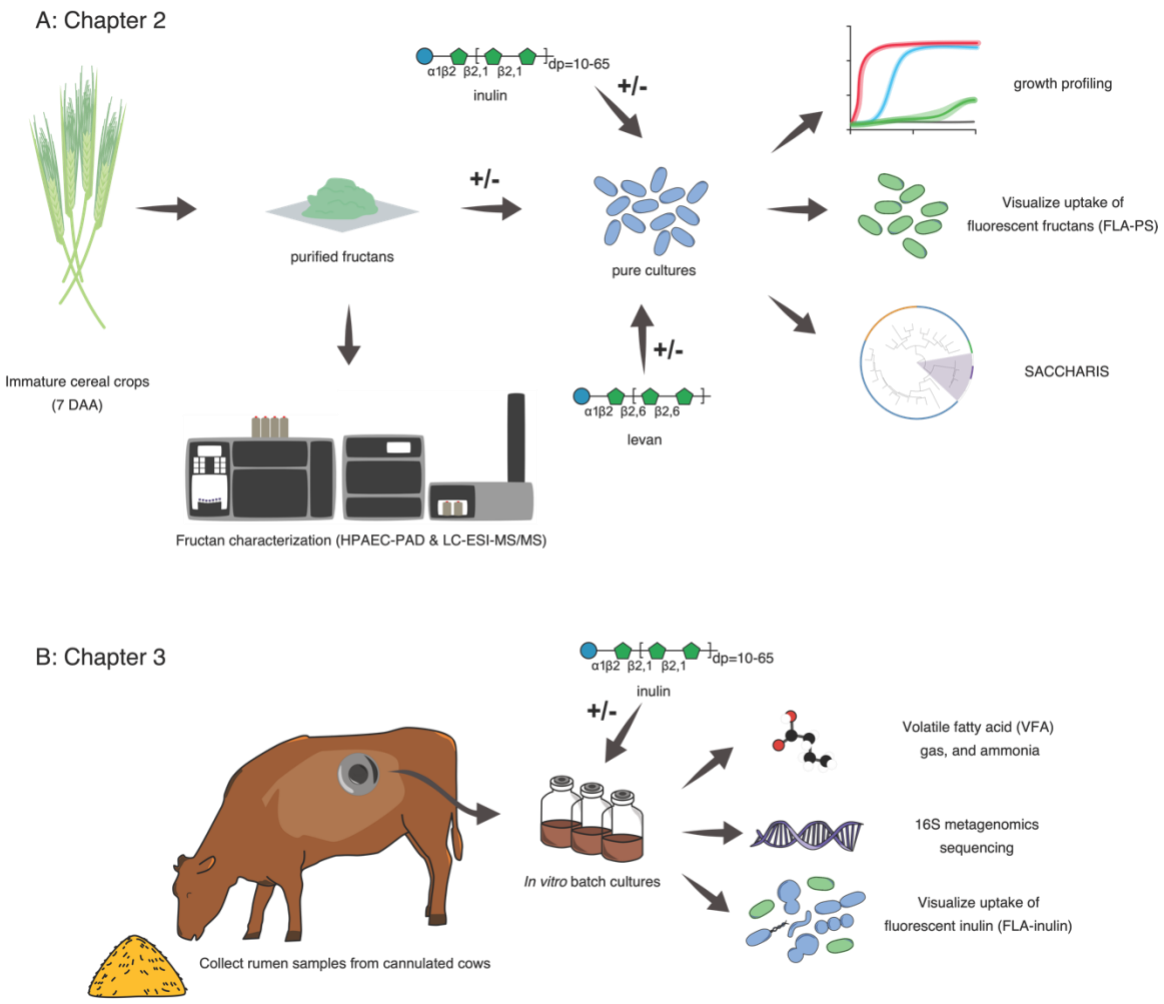

Figure 1.3: Graphical representation of thesis objectives. (A) Assessment of bovine-adapted *Bifidobacterium* and *Lactobacillus* species in utilizing different fructans, including: inulin, levan, and fructans purified from immature winter wheat, spring wheat, and barley kernel and stem fractions (collected 7 DAA). Growth profiling and FLA-PS results will be correlated with the predicted enzymatic activities of GH32s encoded within each species. **(B)** Assessment of the potential prebiotic effects of inulin in non-adapted and inulin-adapted rumen microbial communities using metabolic indicators (production of VFAs, gas, and ammonia), changes in microbiome composition (16S metagenomics) and bacterial interactions with FLA-inulin.

Chapter 2

Mechanistic insight into the propensity of bovine-adapted *Bifidobacterium* and *Lactobacillus* species to catabolize diverse fructans

2.1 Introduction

Fructans are well known for being health-promoting food ingredients for humans and monogastric animals, including companion animals, poultry, swine, and pre-ruminant calves [87, 88]. Fructans are prebiotics, and therefore, reach the intestinal microbiome relatively intact, where they are selectively utilized by beneficial bacteria, including Bifidobacteria and Lactobacilli [89]. Dietary fructan supplementation provides the host with certain health benefits through either direct mechanisms, such as improving lipid profiles [90] and modulating the immune system [91-93], or indirect mechanisms, such as increasing VFA production [94, 95], excluding pathogens [80], and relieving constipation [89]. The DP of fructan chains and linkage positions within the polymer can affect the health benefit outcomes [96, 97].

Inulin is a predominantly linear fructan containing β-2,1 glycosidic linkages and along with its shorter FOS derivatives is the most common fructan. Inulin and FOS extracted from chicory (*Chichorium intybus*) or Jerusalem artichokes (*Helianthus tuberosus*) are typically used as a commercial prebiotic and functional foods. However, several other fructan types exist, which are classified based on their glycosidic linkage composition. Levan is a β-2,6 linked linear fructan synthesized by certain microbes, such as *Erwinia herbicola* and *Zymomonas mobillis* [98, 99] or found in grasses, such as big bluegrass and those belonging to the Poaceae family [36, 100]. Neoseries of inulin and levan contain an internal glucosyl residue and are found within Liliaceae (*e.g.,* onion) and

Asparagaceae (*e.g.,* asparagus) [40] and Poales plants (*e.g.,* oat) [101], respectively. Lastly, graminan-type fructans contain β-2,1 and β-2,6 linkages, giving rise to more complex, branched structures found in certain growth stages of cereal crops (*e.g.,* wheat, barley, rye) [48, 102, 103].

Fructans protect plants against abiotic stresses, such as cold, drought, and high salinity [32, 44, 104]. Within cereal crops, fructans serve as a temporary carbohydrate reserve for approximately 14 DAA until starch accumulation occurs and the plant matures [38]. Fructan abundance varies between different cereal crops, with 18.2% for wheat and 25.1%, for barley reported within the kernel fractions 13 DAA [49]. The presence of fructans has also been identified within the stem and leaf fractions at this growth stage as well [37, 105]. A DP up to 19 has been observed within these immature cereal tissues [102], where in comparison, the average DP for inulin and levan in plants is between 30 and 60 fructosyl residues, and occasionally exceeds 200 [106]. Fructans can be classified according to DP into small (2 – 4), medium (5 – 10), and large (11 – 60 fructosyl residues) [107]. Variation in DPs can affect the fructans prebiotic effects (*e.g.,* changes in community structure). Astó *et al.* [108] found that DP 2 – 8, 10 – 23, and ≥ 23 fructans caused an increased abundance of Actinobacteria members including *Bifidobacterium* spp. within human fecal samples. However, fructans with a DP 2 – 8 had no significant effect on the microbial diversity and failed to stimulate acidification, traits that were seen within samples supplemented with higher DP fructans [108].

Bifidobacterium and *Lactobacillus* are the two main genera impacted by inulin supplementation in human and monogastric animal gut microbiomes [87, 109, 110]; however, the relationship between fructans and these genera within ruminants remains

relatively unexplored. Several members belonging to these genera have been isolated from the bovine rumen, including *B. boum* [111], *B. merycicum* [112], *B. ruminantium* [112], *B. pseudolongum* ssp. *globosum* (*B. globosum*) [113], *L. ruminis* and *L. vitulinus* [114]. Conceivably, combining these probiotic microbes with prebiotic fructans may lead to synergistic effects that can improve cattle health or feed efficiency.

Here, fructans were purified in-house from kernel and stem fractions of immature winter wheat, spring wheat, and barley plants collected 7 DAA, and structural information was obtained through high-performance anion-exchange chromatography with pulsed amperometric detection (HPAEC-PAD) and liquid chromatography electrospray ionization tandem mass spectrometry (LC-ESI-MS/MS). Additionally, four *Bifidobacterium* species: *B. boum* (ATCC 27917)*, B. merycicum* (ATCC 49391)*, B. ruminantium* (ATCC 49390)*, B. globosum* (ATCC 25865); and two *Lactobacillus* species: *L. ruminis* (ATCC 27780) and *L. vitulinus* (ATCC 27783), isolated from bovine rumen samples were assessed for their ability to metabolize different types of fructans. This included fructans purified in-house from kernel and stem fractions of immature winter wheat, spring wheat, and barley plants collected 7 DAA. Fructan catabolism was measured using traditional growth experiments and directly visualized using fluorescent polysaccharides (FLA-PS) of inulin, levan, and fructans from barley kernel and stem fractions. Growth profiles were combined with bioinformatics analysis, using tools such as dbCAN2 [57, 115] and SACCHARIS [56], to identify enzymes predicted to be involved in fructan metabolism

2.2 Results

2.2.1 Utilization of commercial fructans

The ability of rumen-adapted *B. boum, B. ruminantium, B. merycicum, B. globosum, L. vitulinus,* and *L. ruminis* to metabolize different types of fructans was first assessed using commercially available inulin and FOS derived from chicory, and levan synthesized by *Erwinia herbicola*. Of these six species, *B. boum, B. ruminantium, B. merycicum,* and *L. vitulinus* (Figure 2.1A, B, C, F) could utilize FOS when it was provided as the sole carbohydrate source (OD_{600nm} 0.75). The earliest growth on FOS was displayed by *B. merycicum*, which had a lag phase of approximately 9 h; whereas the lag phase was 12 h for *B. ruminantium,* and 18 h for *B. boum* and *L. vitulinus.* Out of the four FOS-utilizing species, *B. boum, B. merycicum,* and *L. vitulinus* were also able to utilize inulin (Figure 2.1A, C, F; OD_{600nm} 0.75), whereas *B. ruminantium* could not (OD_{600nm} < 0.25). *L. vitulinus* was the only specie able to utilize levan, although the growth phase did not commence until after an extended lag phase, approximately 36 h (Figure 2.1F; OD_{600nm} 0.4).

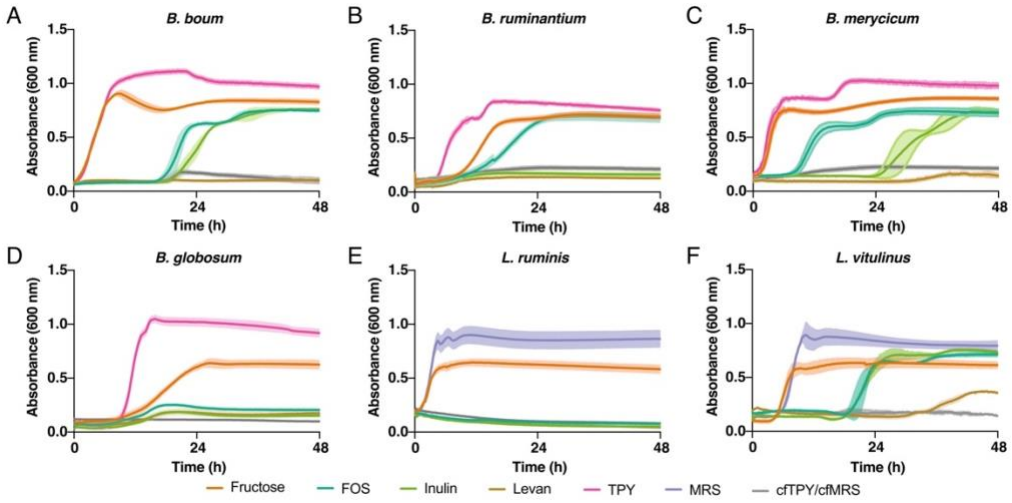

Figure 2.1: Commercial fructan utilization by bovine-adapted *Bifidobacterium* and *Lactobacillus* species. Growth profiles of **(A)** *B. boum,* **(B)** *B. ruminantium,* **(C)** *B. merycicum,* **(D)** *B. globosum,* **(E)** *L. ruminis,* and **(F)** *L. vitulinus* grown in minimalized media containing a 0.5% final concentration of either fructose, fructooligosaccharides (FOS), inulin, or levan as the sole carbohydrate source, or in a rich medium (TPY or MRS) (n = 4).

2.2.2 Visualization of differential FLA-inulin and FLA-levan uptake

Interactions between fructan polysaccharides and *Bifidobacterium* and *Lactobacillus* species, were assessed using fluorescently labelled inulin (FLA-inulin) and levan (FLA-levan). Pure cultures of *B. boum, B. merycicum, L. vitulinus,* and *L. ruminis* were grown on 0.5% inulin or levan for 24 h prior to the addition of 0.2% FLA-inulin or FLA-levan to promote the gene expression of proteins involved in fructan utilization. *B. boum* (Figure 2.2A)*, B. merycicum* (Figure 2.2B)*,* and *L. vitulinus* (Figure 2.2C) showed an interaction with the FLA-inulin as indicated by fluorescent cells seen in the fluorescein isothiocyanate (FITC) channel, whereas *L. ruminis* cells did not become fluorescent after a 1 d incubation (Figure 2.2D). *L. vitulinus* was the only specie that showed uptake of FLA-levan after the 1 d incubation (Figure 2.2C), which was in agreement with its selective growth profile (Figure 2.1F).

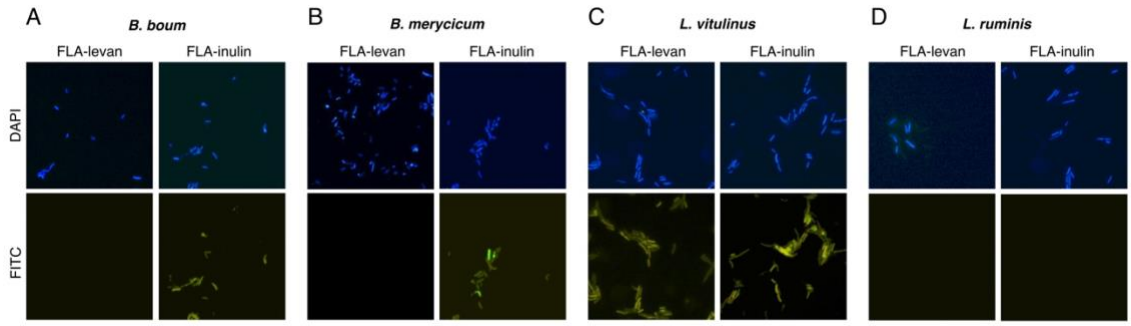

Figure 2.2: Epifluorescence visualization of FLA-inulin and FLA-levan interactions with *Bifidobacterium* and *Lactobacillus* species in pure cultures. (A) *B. boum,* **(B)** *B. merycicum,* **(C)** *L. vitulinus,* and **(D)** *L. ruminis,* where 0.2% FLA-levan incubations (left) and 0.2% FLA-inulin incubations (right) are shown for each species. Samples were primed with 0.5% unlabelled inulin or levan for 24 h prior to 1 d FLA-PS incubations. DAPI was used to stain DNA.

2.2.3 Fructan content within kernel and stem fractions of immature cereal crops

Fructan quantity for the kernel, stem, and leaf fractions of immature winter wheat, spring wheat, and barley was determined using a fructan assay kit (Megazyme K-FRUC) [116]. For spring wheat and barley, fructan was found to be more abundant within the stem fractions, whereas the kernel fraction contained the most fructan for winter wheat (Table 2.1). Amongst the cereal crop fractions assessed, the total fructan content was highest within the barley stem fraction (21.86 ± 0.71 g /100 g dry sample). Fructan quantity within the leaf fraction of each cereal crop was the lowest (~0.6 g/100g dry sample); therefore, the kernel and stem fractions was selected for fructan extractions.

Table 2.1: Fructan quantity within kernel and stem fractions of immature winter wheat, spring wheat, and barley collected 7 DAA where average ± standard deviation is reported (n = 6).

Cereal crop	fraction	Fructan (g/100g dry sample)
Winter wheat	kernel	5.77 ± 0.51
	stem	3.84 ± 0.19
Spring wheat	kernel	3.92 ± 0.31
	stem	18.73 ± 0.74
Barley	kernel	5.52 ± 0.88
	stem	21.86 ± 0.71

To determine the purity and DP range of the fructans isolated from the kernel and stem fractions of immature winter wheat, spring wheat, and barley; purified samples were analyzed by HPAEC-PAD before and after an enzymatic fructan digestion (Figure 2.3). Peaks were observed in each of the cereal crop fractions prior to fructan digestion during 15 – 26 minutes. The DP for each cereal crop fraction is within the 4 – 11 range as determined by comparison to FOS standard peaks. These peaks were absent following enzyme digestion and appeared to be converted to glucose and fructose monosaccharides. Some differences were observed between the plant sources. For winter wheat, smaller DP fructans appear to be present within the stem fraction (Figure 2.3A); whereas for spring wheat and barley, low DP fructans are seen within the kernel fractions (Figure 2.3B, C).

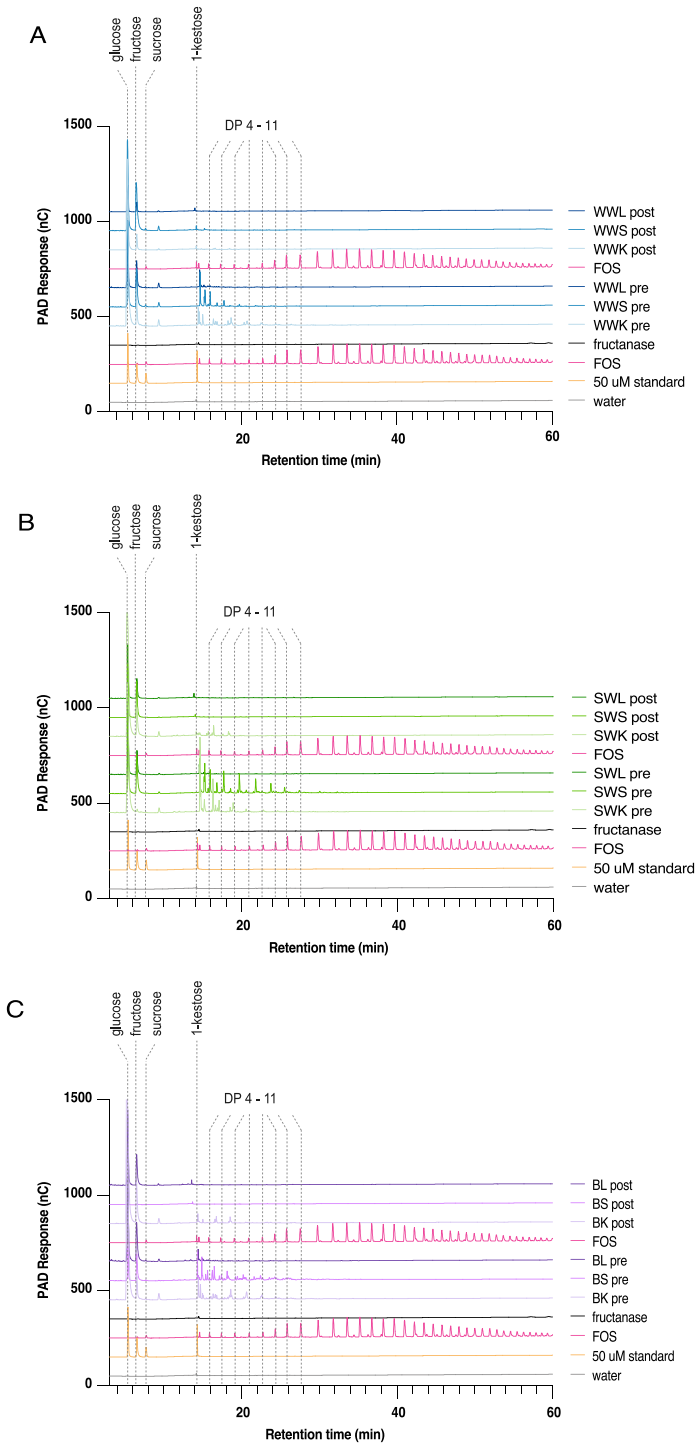
A
glucose
fructose
sucrose
1-kestose
DP 4 - 11
PAD Response (nC)
1500
1000
500
0
20
40
60
Retention time (min)
WWL post
WWS post
WWK post
FOS
WWL pre
WWS pre
WWK pre
fructanase
FOS
50 uM standard
water
B
glucose
fructose
sucrose
1-kestose
DP 4 - 11
PAD Response (nC)
1500
1000
500
0
20
40
60
Retention time (min)
SWL post
SWS post
SWK post
FOS
SWL pre
SWS pre
SWK pre
fructanase
FOS
50 uM standard
water
C
glucose
fructose
sucrose
1-kestose
DP 4 - 11
PAD Response (nC)
1500
1000
500
0
20
40
60
Retention time (min)
BL post
BS post
BK post
FOS
BL pre
BS pre
BK pre
fructanase
FOS
50 uM standard
water

Figure 2.3: **HPAEC-PAD analysis of purified fructans from immature cereal crop fractions collected 7 DAA.** Purified fructans from **(A)** winter wheat, **(B)** spring wheat, and **(C)** barley fractions (kernel, stem, and leaf) were analyzed by HPAEC-PAD using a sodium acetate gradient (0 – 60 min, 10 – 200 mM) with a constant background of 30 mM NaOH. Samples were analyzed before and after being treated with a fructanase enzyme mixture. Peaks appearing within the 15 – 26 min range are proposed fructans. Standard contains 50 μM sucrose, 50 μM 1-kestose, 227 μM fructose, and 227 μM glucose, and was run in parallel.

To provide more structural insights into the purified fructans, the samples were analyzed by LC-ESI-MS/MS using a C18 column to separate the fructans. [117]. Based on the injection of a 1-kestose (DP 3) standard, a DP3 compound eluted between 1.85 – 1.95 min for each cereal crop fraction and was inferred to be 1-kestose (Figure 2.4). The *m/z* values: 503, 665, 827, 989, 1151, 1313, 1475, 1637, 1799, 1961 were used to detect DP 3 – 12 fructans in negative electrospray ionization (ESI) mode. The DP profiles of the different samples varied between cereal crop type and fraction, where a general trend was clearly seen within the spring wheat fractions, that is representative of fructan chain elongation (Figure 2.4B, E) This trend was also seen to a lesser extent within the other cereal crop fraction (Figure 2.4A, C, F); however, the DP profile of winter wheat kernel did not follow, as peaks appear to be scattered throughout the time series (Figure 2.4D).

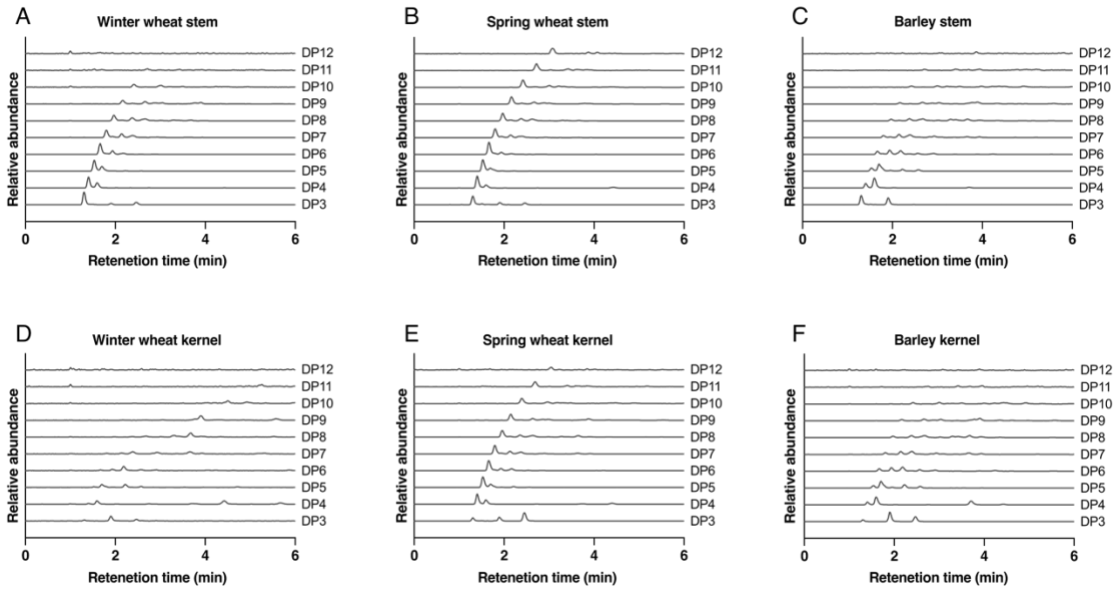

Figure 2.4: Degree of polymerization profiles for the kernel and stem fractions of winter wheat, spring wheat, and barley collected 7 DAA. Extracted ion chromatograms for (A) winter wheat stem, (B) spring wheat stem, (C) barley stem, (D) winter wheat kernel, (E) spring wheat kernel, and (F) barley kernel fractions, at 503, 665, 827, 989, 1151, 1313, 1475, 1637, 1799, 1961 *m/z* values corresponding to DP 3 – 12 fructans.

2.2.4 Utilization of purified fructans from immature cereal crops

The ability of *B. boum, B. merycicum,* and *L. vitulinus* to utilize fructans purified from the kernel and stem fractions of immature winter wheat, spring wheat, and barley was assessed in cultures containing carbohydrate-free (cf) trypticase phytone yeast extract (TPY) or De Man, Rogosa, and Sharpe (MRS) media with the purified fructans provided as the sole carbohydrate source. Within the first 24 h of incubation, all three species showed utilization of fructans from each cereal crop fraction (Figure 2.5A, B, C). The area under the curve (AUC) was calculated for the first 18 h of each growth curve. From the growth profile of *B. boum,* growth on SWS resulted in the highest AUC value out of the fructan sources examined, whereas the growth of this specie on WWS was the lowest (Figure 2.5D). For *B. merycicum,* growth on BK resulted in the highest AUC, whereas both SWS and SWK fractions had the lowest value (Figure 2.5E). The growth of *L. vitulinus* on any of the purified fructan sources resulted in a similar growth profile to when fructose is the sole carbon source. For this specie, growth on WWK resulted in the lowest AUC value (Figure 2.5F).

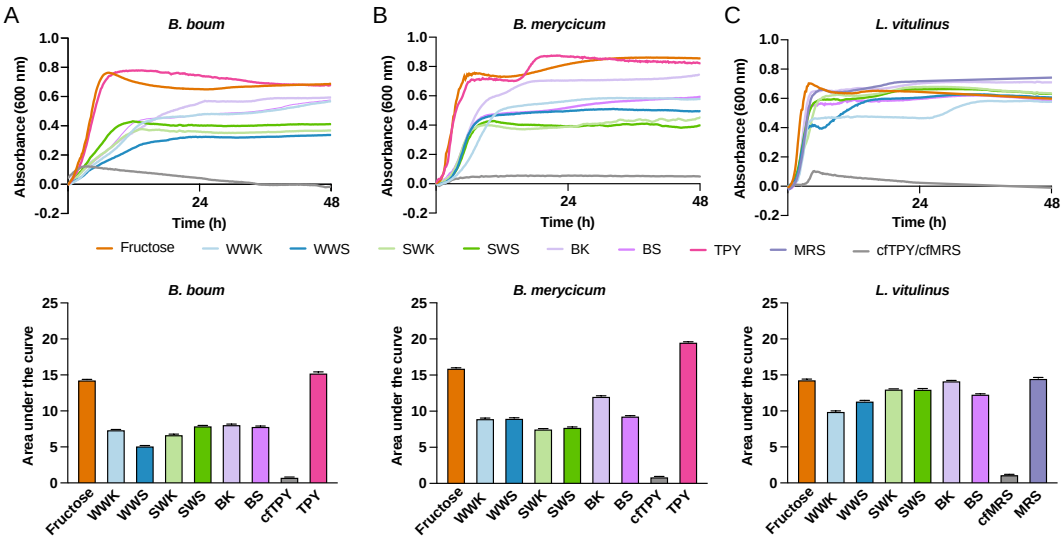

Figure 2.5: Utilization of fructans isolated from immature cereal crop fractions by bovine-adapted *Bifidobacterium* and *Lactobacillus* species. Growth profiles (48 h, top) and corresponding area under the curve (AUC) plots (18 h, bottom) for **(A)** *B. boum,* **(B)**, *B. merycicum,* and **(C)** *L. vitulinus,* when fructans isolated from kernel and stem fractions of winter wheat, spring wheat, and barley samples were collected 7 DAA.

2.2.5 Visualization of FLA-BK and FLA-BS utilization

Fluorescently labelled conjugates of purified fructans from barley kernel and stem fractions (FLA-BK and FLA-BS) were used to visualize interactions occurring with *Bifidobacterium* and *Lactobacillus* species in pure cultures. Samples were incubated with 0.2% FLA-BK or 0.2% FLA-BS, to assess if fructans sourced from different regions of the plant resulted in diverse uptake responses. The rate of uptake was also assessed by examining aliquots taken at the 5 min and 1 h time points. After 5 min of FLA-PS incubations, *B. boum, B. merycicum, L. ruminis,* and *L. vitulinus* displayed utilization of both FLA-BK and FLA-BS (Figure 2.6), whereas FLA-BK and FLA-BS utilization by *B. ruminantium* and *B. globosum* occurred later at the 1 h time point (Figure 2.6B, D, H, J). Samples taken before FLA-BK or FLA-BS exposure showed no fluorescence in the FITC channel.

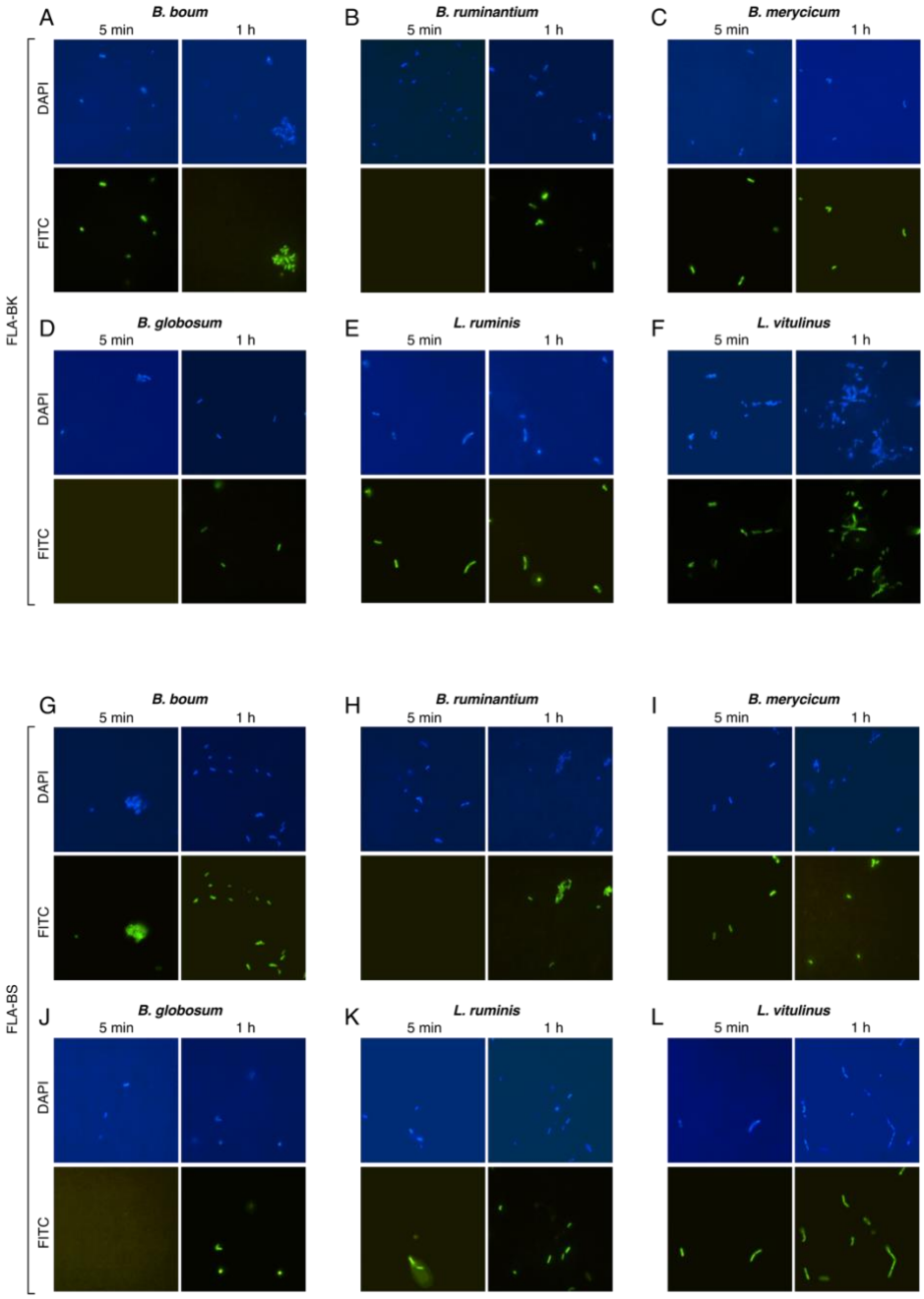

Figure 2.6: Epifluorescence visualization of FLA-BK and FLA-BS interactions with *Bifidobacterium* and *Lactobacillus* species in pure cultures (A) *B. boum,* **(B)** *B. ruminantium,* **(C)** *B. merycicum,* **(D)** *B. globosum* **(E)** *L. ruminis,* and **(F)** *L. vitulinus* incubations with 0.2% FLA-BK. **(G)** *B. boum,* **(H)** *B. ruminantium,* **(I)** *B. merycicum,* **(J)** *B. globosum* **(K)** *L. ruminis,* and **(L)** *L. vitulinus* incubations with 0.2% FLA-BS. Samples were taken 5 min and 1 h after incubation with the fluorescent conjugates. DAPI was used to stain DNA.

2.2.6 Comparative analysis of GH32 enzymes

Assembled genome sequences of the six species were retrieved from the NCBI assembly database, and the total CAZyme content of each specie (*i.e.,* CAZome fingerprinting) was determined using the dbCAN2 meta server. CAZome comparisons revealed that *B. globosum* encoded 40 GH enzymes, including 17 GH13s and 7 GH43s. To investigate the potential for fructan metabolism, sequences encoding GH32 members were analyzed at higher resolution; GH32s have been shown to be active on β-2,1 and β-2,6 glycosidic linkages found within fructans. *L. vitulinus* possesses 5 GH32s (NZ_JNKN01000017.1_4, NZ_JNKN01000049.1_5, NZ_JNKN01000007.1_60, NZ_JNKN01000025.1_18, and NZ_JNKN01000025.1_23), the highest abundance out of the six species (Supplementary Table 1). Two GH32s were encoded within the genome of *B. merycicum* (NZ_FQTX01000003.1_36 and NZ_FQTX01000001.1_82), whereas the other four species contained a single GH32. InterProScan [118] was used to identify the full length structure of the polypeptides; one GH32 (NZ_JNKN01000017.1_4) from *L. vitulinus* was found to be multi-modular as it contained a family 66 carbohydrate binding module (CBM66) and was predicted to be secreted (Figure 2.7B).

The GH32 enzymes of each species were collectively analyzed by SACCHARIS [56] to determine sequence relatedness and predict enzyme activity. Each GH32 was integrated into a phylogenetic tree constructed with GH32s that were previously biochemically characterized. From this alignment, almost all of the predicted GH32s from the rumen-adapted *Bifidobacterium* and *Lactobacillus* species were predicted to possess β-fructofuranosidase (EC 3.2.1.26) activity. Interestingly, the GH32 belonging to *L. vitulinus* containing the CBM66 (NZ_JNKN01000017.1_4) displayed the most sequence

divergence and was partitioned within a clade comprised of levan-specific enzymes (*i.e.,* endo-levanase (EC 3.2.1.65), 6-levanbiohydrolase (EC 3.2.1.64), and levan fructantransferases (4.2.2.16)) and one fructan β-fructosidase (EC 3.2.1.80; Figure 2.7A).

Alignment of the GH32 amino acid sequences using MUSCLE [119] revealed varying levels of sequence conservation amongst the six species. Highest conservation was seen between *B. ruminantium* (NZ_JHWQ01000002.1_227) and *B. merycicum* (NZ_FQTX01000001.1_82) at 90% similarity (496 aa, Table 2.2). The single GH32 encoded within the genome of *L. ruminis* (NZ_CP007457.1_1300) was found to be ~74% identical to these two GH32s (532 aa), and all three of these GH32s are clustered together within a clade (Figure 2.7A). The other identified GH32 belonging to *B. merycicum* (NZ_FQTX01000003.1_36) was closest related to the GH32 from *B. boum* (NZ_JABAGJ010000007.1_104) (Figure 2.7A); there was ~51% identity between these two members (486 aa). Of note, two GH32s belonging to *L. vitulinus* (NZ_JNKN01000017.1_4, NZ_JNKN01000049.1_5) and the one from *B. globosum* (NC_015975.1_1878) showed the most divergence to the other GH32s being analyzed (20 – 37%; Table 2.2).

Many of the gene clusters involved in fructan metabolism of the *Bifidobacterium* species show a related composition containing a LacI-type regulator and an ABC transporter; however, the gene orientation and copy number does vary between the species. Most *Bifidobacterium* species contain a major facilitator superfamily (MFS) transporter upstream of the ABC transporter. For the *Lactobacillus* species, other transporter classes, including phosphotransferase system (PTS) enzyme IIC component, were seen (Supplementary Figure 1).

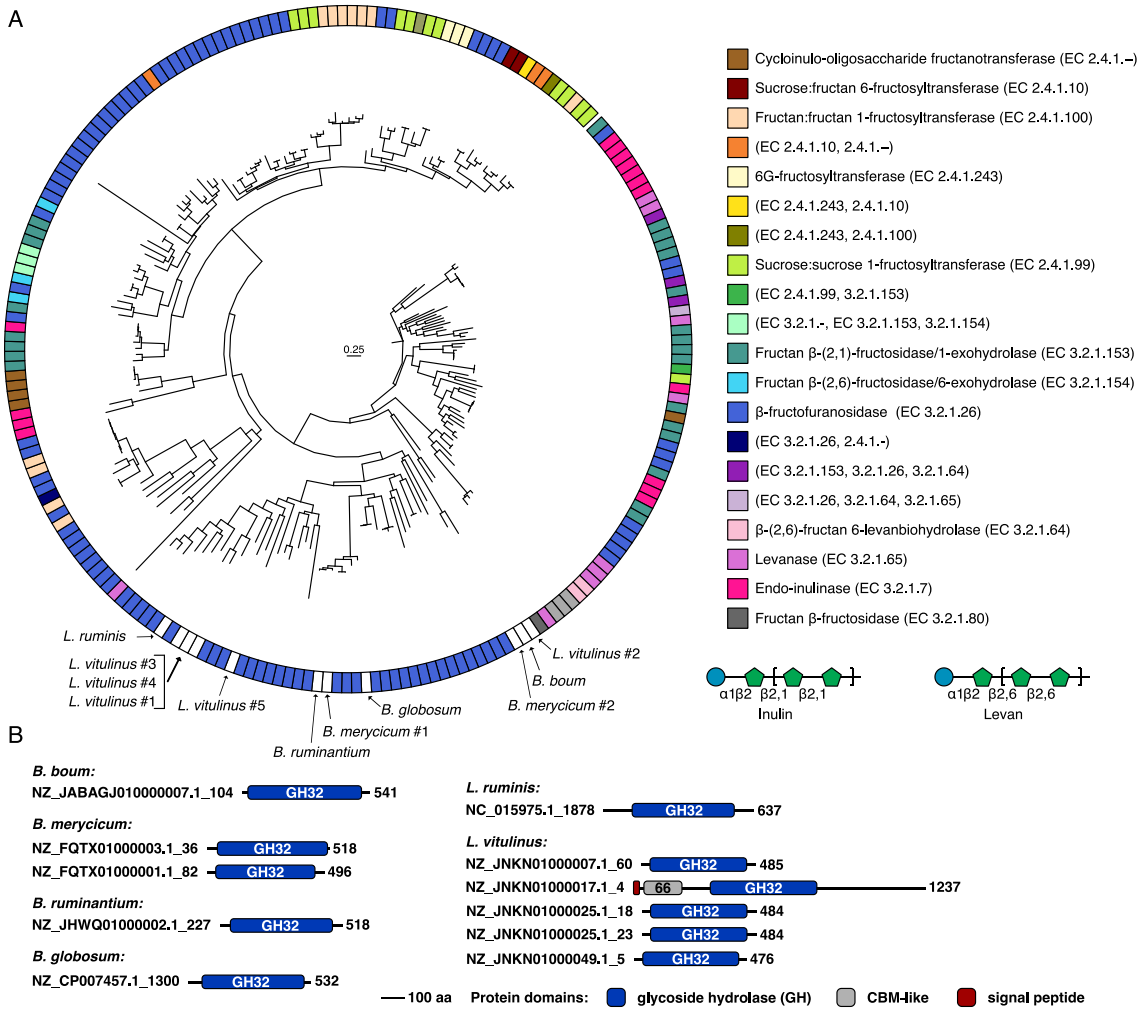

Figure 2.7: Predicted enzymatic activities of GH32s belonging to bovine-adapted *Bifidobacterium* and *Lactobacillus* species. (A) phylogenetic tree of characterized GH32s and sequences encoding GH32s from bovine-adapted *Bifidobacterium* and *Lactobacillus* species, generated with SACCHARIS [56]. **(B)** GH32 protein modules for each species, analyzed using InterProScan [118].

Table 2.2: Percent identity matrix of the GH32 amino acid sequences from bovine-adapted *Bifidobacterium* and *Lactobacillus* species generated by MUSCLE [119], where grey shading represents conservation ≥ 50%.

	1	2	3	4	5	6	7	8	9	10	11
1	- - -	51.3	20.3	25.2	26.2	27.0	20.0	21.3	22.9	20.4	20.4
2	51.3	- - -	21.8	24.9	27.1	27.5	21.0	20.9	21.2	19.8	19.8
3	20.3	21.8	- - -	25.5	26.5	26.1	21.5	21.1	20.0	22.2	22.4
4	25.2	24.9	25.5	- - -	74.8	73.8	24.2	25.7	24.3	25.2	25.2
5	26.2	27.1	26.5	74.8	- - -	90.5	25.5	25.7	25.6	25.4	26.1
6	27.0	27.5	26.1	73.8	90.5	- - -	25.9	24.9	26.2	25.6	26.5
7	20.0	21.0	21.5	24.2	25.5	25.9	- - -	31.2	28.6	27.3	28.0
8	21.3	20.9	21.1	25.7	25.7	24.9	31.2	- - -	37.3	34.4	35.2
9	22.9	21.2	20.0	24.3	25.6	26.2	28.6	37.3	- - -	52.4	50.5
10	20.4	19.8	22.2	25.2	25.4	25.6	27.3	34.4	52.4	- - -	63.5
11	20.4	19.8	22.4	25.2	26.1	26.5	28.0	35.2	50.5	63.5	- - -

1 = *B. boum* (NZ_JABAGJ010000007.1_104)
2 = *B. merycicum* (NZ_FQTX01000003.1_36)
3 = *L. vitulinus* (NZ_JNKN01000017.1_4)
4 = *L. ruminis* (NZ_CP007457.1_1300)
5 = *B. merycicum* (NZ_FQTX01000001.1_82)
6 = *B. ruminantium* (NZ_JHWQ01000002.1_227)
7 = *L. vitulinus* (NZ_JNKN01000049.1_5)
8 = *B. globosum* (NC_015975.1_1878)
9 = *L. vitulinus* (NZ_JNKN01000007.1_60)
10 = *L. vitulinus* (NZ_JNKN01000025.1_18)
11 = *L. vitulinus* (NZ_JNKN01000025.1_23)

2.3 Discussion

Despite the documented prebiotic effects associated with fructans and their use historically as functional food ingredients, interactions between *Bifidobacterium* spp. and *Lactobacillus* spp. in response to varying fructan types and chain lengths has yet to be fully evaluated. For animal health and nutrition, the combination of probiotics and prebiotics, or synbiotics, may prove to be an important tool for maintaining or improving the health and growth performance of animals [67]. Within this study, several types of fructans, including inulin, levan, and fructans from immature cereal crops (7 DAA), that were purified and structurally characterized, were used to assess the capacity of six bovine-adapted *Bifidobacterium* and *Lactobacillus* species to metabolize fructans.

The amount of fructan present within cereal crops is dependent on several factors, including the genetics, growth stage, and tissue type. Fructan abundance is highest when the plant is immature, where maximum values of 18.2%, 25.1%, and 30.0% have been reported for wheat, barley, and rye grains collected 13 DAA, respectively [120]. In comparison, fructan levels within the wholegrains of mature cereal crops are between 0.9 – 4.2% for barley [48], 0.6 – 2.6% for wheat [121], and 4.4 – 6.6% for rye [103]. Within this study, the fructan abundance varied between the crop type and fraction assessed, with the highest fructan content contained within the stem fraction of barley (21.86 ± 0.71%; Table 2.1). In relation to the fructan values reported by Nardi *et al.* [120] and Verspreet *et al.* [38], the amounts reported within this study are low. However, the breeding line or cultivar of the crop as well as environmental factors (*e.g.,* irrigation) can significantly affect fructan concentrations [48, 122], and may explain some of the fructan content

variations seen between studies. Further investigation of how these levels vary between plants and growth conditions will provide more insight into fructan biology.

Within immature cereal crops, a wide range of fructans are present as multiple isomeric conformations can be seen in each DP. A DP range of 3 – 12 was determined through HPAEC-PAD and LC-ESI-MS/MS analyses for fructans purified from immature cereal crop fractions (Figure 2.3 and 2.4). However, the relative abundance of different DPs varied between the crop types, as a higher abundance of DP 9 – 12 was seen within spring wheat (Figure 2.4). 1-kestose was determined to be present within all 6 cereal crop fractions (Figure 2.4). This trisaccharide contains a β-2,1 glycosidic linkage, and is the precursor for inulin synthesis [39]. Two other peaks corresponding to a 503 *m/z* value can also be seen in each sample (Figure 2.4). Based on previous literature [33, 102, 117], these peaks may represent 6-kestose and 6G-kestose, the initial trisaccharides required for the elongation of levan and neo-fructan series, respectively. However, the identity of these DP 3 peaks cannot be fully confirmed from this analysis as limited fructan standards are available and linkage analysis (*i.e.,* methylation GC-MS methods) has not been completed on these samples at this time.

Several factors can affect the ability of bacteria to utilize fructans, including the fructan type and DP. The propensity of *Bifidobacterium* and *Lactobacillus* species isolated from the GI tract of humans to utilize different fructan types, including small mixed-linkage (β-2,1 and β-2,6) neoseries fructans derived from *Agave* spp., was examined by Mueller *et al.* [97]. Several DP ranges of agave fructans and inulin were tested, where *B. animalis* ssp. *lactis* BB12 (DSM 15954), *L. reuteri* (ATCC 55730), *L. acidophilus* LA-5 (DSM 13241), *L. rhamnosus* GG (ATCC 53103), and several *L.*

paracasei ssp. *paracasei* strains (ATCC 55544, DN114001, and DSM 20315) showed growth on agave fructans ranging from DP 3 – 11 [97]. However, their responses to other fructan sources varied as *L. rhamnosus* GG, *B. animalis* ssp. *lactis* BB12, and *L paracasei* DN114001 showed delayed growth when grown on inulin with an average DP > 8 [97]. Similarly, within this study, bovine-adapted *Bifidobacterium* and *Lactobacillus* species differed in their utilization of commercial fructans (*i.e.,* FOS, inulin, and levan; Figure 2.1) but were able to utilize smaller fructans from immature cereal crops (Figure 2.5, DP 3 – 12). As human and bovine-adapted *Bifidobacterium* and *Lactobacillus* species display similar growth profiles for different fructan DP ranges, utilization of smaller fructans may be preferred regardless of glycosidic linkages as these substrates may be directly imported into the cells; whereas with the longer chained commercial fructans, the activity of extracellular enzymes is required to depolymerize the fructans first, and the enzymatic specificity dictates which larger fructans can be utilized.

The development of FLA-PS has given rise to rapid assessments of carbohydrate metabolism and phenotypic differences within a community [86, 123]. Previously, FLA-PS have been applied to Gram-negative (e.g., *Bacteroides thetaiomicron* VPI-5482, *Gramella forsetti* KT0803, *Cantenovulum* spp.) and *Planctomycetes* spp. [84-86], which resulted in a halo-like phenotype because the fluorescent conjugates accumulate within the periplasmic space [85, 86]. This is the first time FLA-PS have been applied to pure cultures of Gram-positive bacteria. (Figure 2.2 and 2.6). There was at least 1 positive FLA-interaction seen with each FLA-PS probe, where each specie showed differential specificities towards the FLA-PS probes. For instance, *L. ruminis* imported FLA-BK (Figure 2.6E) and FLA-BS (Figure 2.6K) but not FLA-inulin or FLA-levan (Figure 2.2D). *L. vitulinus* was the only specie to import all 4 probes (FLA-inulin, FLA-levan: Figure

2.2C; FLA-BK: Figure 2.6F; FLA-BS: Figure 2.6L). As the genomes of *B. boum* and *B. merycicum* do not encode extracellular GH32s, it was surprising to see both species import polymerized forms of inulin. Potentially, this result, and results seen in other studies [111, 112] was because there is a range of DPs present within the inulin sample, the smaller of which are more easily transported, and/or differences in the ABC transporter specificity may differentiate between the size of inulin that is imported into the cell for depolymerization.

Differences in the propensity of *Bifidobacterium* and *Lactobacillus* species to metabolize distinct fructans appears to vary between species and be dependent on the fructan structure. For instance, the presence of 5 GH32s within the genome of *L. vitulinus* is in agreement with the observation that this specie can grow on both β-2,1 and β-2,6 fructans (Figure 2.1F). Notably, one of the GH32s belonging to *L. vitulinus* (NZ_JNKN01000017.1_4), clusters with enzymes previously characterized to hydrolyze levan (Figure 2.7A). This closest homolog is fruA from *Streptococcus mutans* GS-5 (36% identity, 1 237 aa, GenBank AAA26889.1) [124, 125]. FruA has been previously characterized as a fructan β-fructosidases (EC 3.2.1.80), that could hydrolyze terminal residues in inulin and levan at the non-reducing end [125]. As this is also the predicted activity for GH32 (NZ_JNKN01000017.1_4), the presence of a CBM66 in each of these proteins is predicted to potentiate enzyme function by binding to terminal fructosyl residues [126]. Interestingly, the endo-acting levanases within this clan did not contain a CBM66, which suggests there may be a difference in the accessibility or solubility of these two fructans.

Apart from the multi-modular GH32 (NZ_JNKN01000017.1_4) with predicted β-fructosidase activity, all other GH32s were single modules with predicted β-fructofuranosidase (EC 3.2.1.26) activity (Figure 2.7). The *B. boum* (NZ_JABAGJ010000007.1_104) GH32 and *B. merycicum* (NZ_FQTX01000003.1_36) GH32 shared a node within the GH32 phylogenetic tree (Figure 2.7A). There was 51% identity between these two enzymes (486 aa, Table 2.2), and these two species showed similar genomic architectures for fructan metabolism (Supplementary Figure 1). In agreement with previous studies [127, 128], both species showed utilization of FOS and inulin, where *B. merycicum* had a shorter lag time for FOS utilization (9 h, Figure 2.1C) which may result from the presence of 2 GH32s within its genome (Figure 2.7A). *L. vitulinus, B. boum,* and *B. merycicum* displayed quick growth responses to fructans purified from immature cereal crops (Figure 2.5 and 2.6). As these fructans were relatively small (DP 3 – 12) in comparison to the FOS standard (DP 4 – 38) seen in Figure 2.3, rapid growth responses may indicate a preference for smaller fructans.

While fructan utilization by *Bifidobacterium* and *Lactobacillus* species was found to be rapid when fructans purified from immature cereal crops were used, it is unclear how these fructans would be utilized in a mixed community, and if any beneficial effects of the probiotic species would be seen. In a study conducted by Jenkins *et al.* [129] using human fecal samples, it was found that fructans purified from immature barley kernels and wheat stems (14 DAA; DP < 11; 1.5%), resulted in similar fermentation properties with inulin and FOS, and production of butyrate and propionate was favoured. However, this study [129] did not examine other metabolic responses, such as gas production, and compositional changes to the microbiome.

Mature cereal crops represent the main dietary source of fructans for humans [39]; however, 30 – 60% of fructans can be lost during food processing (*e.g.,* dry heating, yeast fermentation during bread making) [130-132]. Cereal crops are also routinely used in ruminant feed, where cattle are presumably consuming available fructans as well. As environmental and genetic factors dictate fructan abundance, some crop producers are evaluating breeding prospects for increasing fructan content [35]. Increased fructan amount would not only be beneficial for human and animal nutrition, but also for crop health as fructans can aid in preventing yield losses [35].

2.4 Conclusion

The ability of bovine-adapted *Bifidobacterium* and *Lactobacillus* species to metabolize fructans was found to be dependent on the fructan linkage composition and DP, and the predicted activity of their encoded GH32 sequences. *B. boum*, *B. merycicum*, and *L. vitulinus* could utilize inulin and FOS, but *L. vitulinus* was the only specie able to grow on levan, albeit after an extended lag phase. All species grew on fructans purified from immature barley kernel and stem fractions (DP 3 – 12), indicating they may function as a potential probiotic. The interaction between fructans and probiotic bacteria in the rumen microbiome, which is a highly competitive ecosystem, remains to be determined. It is unclear if the early response by some probiotic species on cereal drop-derived fructans will occur to the same extent within the rumen microbiome and if or how these small fructans will be benefit the host. These findings may contribute to future improvements in fructan development by providing on-farm sources of prebiotics or prebiotics with specialized chemistries for animal intestinal health and nutrition.

2.5 Materials and methods

2.5.1. Collection and storage of immature winter wheat, spring wheat, and barley crops

Above ground biomass of winter wheat, spring wheat, and barley was collected from fields at the Lethbridge Research and Development Centre (Lethbridge, AB, Canada) approximately 7 DAA. Each cereal crop was divided into kernel, stem, and leaf fractions where fractions were flash frozen and lyophilized. Samples were then ball-milled with a RETSCH MM 400 Mixer Mill (30 Hz, 3 min; Fisher Scientific 08418241) and powders were stored at room temperature until further use.

2.5.2 Fructan quantification

To determine the amount of fructan present within the kernel, stem, and leaf fractions of winter wheat, spring, wheat, and barley, a previously defined protocol was used [116] with minor modifications. Briefly, 0.1 g of ball-milled sample was suspended in 1 mL distilled water. Solution was vortexed and then 14 mL of boiling distilled water was added. Solutions were incubated at 80 °C for 16 h with gentle shaking, and then cooled to room temperature and centrifuged at 13 000 *x g*, 5 min and the supernatant was recovered. 0.2 mL of a sucrase/amylase mixture (2 U sucrase, 22 U β-amylase (*Bacillus cereus*), 4.5 U pullulanase (*Bacillus licheniformis*), and 45 U maltase (yeast) in 100 mM sodium maleate buffer, pH 6.5) was added to 0.2 mL of the supernatants. These solutions were incubated at 30 °C for 30 min. 0.2 mL of freshly made alkaline borohydride (10 mg/mL sodium borohydride in 50 mM NaOH) was added. Solutions were briefly vortexed and incubated at 40 °C for 30 min before 0.5 mL of 200 mM acetic acid was added. The resulting solution was divided into 0.2 mL aliquots where 0.1 mL of a

fructanase solution (363 U exo-inulinase, 11 U endo-inulinase, and 7 U endo-levanase in 100 mM sodium acetate buffer, pH 4.5) was added to three 0.2 mL aliquots, and 0.1 mL of 100 mM sodium acetate buffer, pH 4.5 was added to the other two 0.2 mL sample aliquots as controls. Solutions were incubated at 40 °C for 30 minutes before 5 mL of a *para*-hydroxybenzoic acid hydrazide (PAHBAH, Sigma H9882) working solution (20 mL of 5% PAHBAH, 0.05% HCl, and 180 mL of 1.2% trisodium citrate dihydrate, 0.1% $CaCl_2 \cdot 2\ H_2O$, 2% NaOH) was added. Samples were incubated in a boiling water bath for 6 min before the absorbance at OD_{410nm} was measured using a plate reader. The total fructan content was calculated using the Megazyme Mega-Calc™ Excel-based calculator downloaded from the website (https://www.megazyme.com).

2.5.3 Purification of fructans from immature cereal crop fractions

For each extraction, 1.5 g of ball-milled sample was suspended in 5 mL of distilled water and vortexed to mix. 45 mL of boiling distilled water was added, and solutions were incubated at 80 °C for 16 h with gentle stirring. Solutions were cooled and centrifuged at 13 000 *x g*, 5 min. The supernatant was collected and 2 mL of amylase solution (1 000 U mL^{-1}, thermostable *Bacillus licheniformis* α-amylase; Megazyme E-BLAAM; in 100 mM sodium acetate pH 5.0, 5 mM $CaCl_2$) was added per 40 mL of supernatant. Solutions were incubated at 40 °C for 16 h with gentle stirring. The temperature was lowered to 30 °C and 0.2 mL α-galactosidase (200 U mL^{-1}, *Aspergillus niger*, Megazyme E-AGLAN) and 0.2 mL sucrase/amylase mixture (2 U sucrase, 22 U β-amylase (*Bacillus cereus*), 4.5 U pullulanase (*Bacillus licheniformis*), and 45 U maltase (yeast) in 100 mM sodium maleate buffer, pH 6.5) were added and solutions were incubated for an additional 16 – 20 h. The resulting destarched solution was centrifuged

at 3 000 *x g*, 5 min, filtered (0.45 μm) and run through a (3 cm x 14 cm) column containing 5 g Supelclean™ ENVI-Carb™ solid phase extraction (SPE) bulk packing (Sigma 57210) conditioned with 2 column volumes (CV) of 95% ethanol, and equilibrated with 2 CV of distilled water prior to sample loading. Column was washed with 1 CV of distilled water and 1 CV of 5% ethanol before FOSs were eluted off with 2 CV of 30% ethanol. Elution fractions were dried to completeness using a sample concentrator (35 °C), then resuspended in distilled water and lyophilized.

2.5.4 High-performance anion-exchange chromatography with pulsed amperometric detection (HPAEC-PAD)

HPAEC-PAD was performed using a Dionex ICS-3000 chromatography system (Thermo Scientific) equipped with an autosampler and a pulsed amperometric detector (PAD). 10 μL of diluted sample were injected onto an analytical (3 x 150 mm) PA200 column (Thermo Scientific) and eluted at a 0.5 mL min^{-1} flow rate with a sodium acetate gradient (0 to 60 min, 10 – 200 mM) with a constant solvent of 30 mM NaOH. A 0.1% FOS solution, and a standard mixture composed of 50 μM sucrose, 50 μM 1-kestose, 227 μM fructose, and 227 μM glucose, were run in parallel. Data was collected using the Chromeleon chromatography management system and plotted using GraphPad Prism version 9.1.1.

2.5.5 Liquid chromatography-electrospray ionization-tandem mass spectrometry (LC-ESI-MS/MS)

Purified fructans from winter wheat, spring wheat, and barley kernel and stem fractions were diluted to 250 μM with distilled water and filtered (0.2 μm). Fructan separation was performed using an InfinityLab Poroshell 120 SB-C18 column (2.1 mm x 150 mm, 2.7 μm; Agilent 683775-902) where 0.1% formic acid was used at the solvent. Fructans were detected with a Finnigan LTQ mass spectrometer (Thermo Scientific). Electrospray ionization was conducted in negative mode and charged analytes were screened over a mass range of 50 to 2 000 *m/z*. For MS^2 analysis, ions were isolated in quadrupole mass analyzer with a window of 0.5 *m/z*. Collision induced dissociation was performed with 35% collision energy. Data was collected in centroid mode and analyzed with Xcalibur 3.1 software Qual Browser.

2.5.6 Bovine-adapted *Bifidobacterium* and *Lactobacillus* species and culture conditions

Bifidobacterium boum (ATCC 27917), *Bifidobacterium pseudolongum* ssp. *globosum* (ATCC 25865), *Bifidobacterium merycicum* (ATCC 49391), *Bifidobacterium ruminantium* (ATCC 49390), *Lactobacillus vitulinus* (ATCC 27783), and *Lactobacillus ruminis* (ATCC 27780) were purchased from Cedarlane Laboratories (Burlington, ON). *Bifidobacterium* species were inoculated in Trypticase-phytone-yeast extract (TPY) medium: 1.5% glucose, 1% Bacto™ Tryptone (BD 211705), 0.5% neutralized soya peptone (Oxoid LP0044), 0.25% bacteriological grade yeast extract (VWR J850), 0.2% dipotassium phosphate, 0.05% L-cysteine, 0.05% magnesium chloride, 0.025% zinc sulfate, 0.015% calcium chloride, 0.001% ferric chloride. *Lactobacillus* species were

inoculated in De Man, Rogosa and Sharpe (MRS) medium: 5.1% MRS Broth (Sigma 69966), 1 mL/L Tween® 80 (Sigma P-8074) [133]. Cultures were incubated anaerobically (atmosphere: 85% N_2, 10% CO_2, 5% H_2) within a vinyl anaerobic chamber (Coy Lab Products) set to 37 °C for 48 hours.

2.5.7 Growth profiling of bovine-adapted *Bifidobacterium* and *Lactobacillus* species

B. boum, B. merycicum, B. ruminantium, B. globosum were cultured in TPY medium, whereas *L. vitulinus* and *L. ruminis* were cultured in MRS medium. All incubations were performed in an anaerobic chamber (atmosphere: 85% N_2, 10% CO_2, 5% H_2) at 37 °C overnight. The overnight cultures (OD_{600nm} 1.0 – 1.3) were centrifuged at 4 000 *x g*, 10 min and then washed with carb-free media before being diluted to an OD_{600nm} of 0.2 in either 2X cfTPY: 1 % Bacto™ Tryptone (BD 211705), 1% neutralized soya peptone (Oxoid LP0044), 0.5% yeast extract bacteriological (VWR J850), 0.4% potassium phosphate dibasic anhydrous (VWR 0705), 0.1% L-cysteine, 0.1% magnesium chloride anhydrous, 0.05% zinc sulfate, 0.03% calcium chloride, 0.002% ferric chloride; or 2X cfMRS medium: 2% Bacto peptone (BD 211677), 1% yeast extract bacteriological (VWR J850), 1% sodium acetate, 0.4% ammonium citrate, 0.4% potassium phosphate, 0.04% magnesium sulphate, 0.01% manganese sulphate, 2 mL/L Tween® 80 (Sigma P-8074); for the *Bifidobacterium* and *Lactobacillus* species, respectively.

Solutions of 1% (w/v) in distilled water were made for fructose (Sigma F0127), FOSs from chicory (Sigma F8052), inulin from chicory (Sigma I2255), levan from *Erwinia herbicola* (Sigma L8647), and the purified fructans from the kernel and stem fractions of winter wheat, spring wheat, and barley (7 DAA). Wells of a 96-well microtiter plate (Greiner CELLSTAR®, Sigma M0437) were filled with 100 µL of

sterilized 1% carbohydrate; along with 100 µL of bacterial inoculant (OD_{600} 0.2). Negative control wells consisted of 100 µL 2X cf media combined with 100 µL 1% carbohydrate, and were used to normalize growth curves and AUC values. Additional media controls were conducted, where the growth of each specie was assessed in rich media (TPY or MRS) and the respective cf media version. Polyurethane Breath-Easy® sealing membranes (Sigma Z380059) were used to seal plates. Absorbance (600 nm) of each well was measured with a Cerillo stratus plate reader (Charlottesville, VA, USA) every 10 min for 48 h. Mean (± standard deviation) and AUC for each condition (n = 4) was plotted using GraphPad Prism version 9.1.1.

2.5.8 Levan acid hydrolysis

50 mg of levan was dissolved in 5 mL 0.2 M HCl. Solution was incubated at 50 °C for 20 min before the reaction was neutralized using NaOH. Monosaccharides and small oligosaccharides were removed from solution by centrifugation at 3 000 *x g,* 30 min using Sartorius Vivaspin 15R columns (5 000 MWCO; VS15RH11). Flow through was removed and columns were topped off with distilled water to wash hydrolyzed sample. Wash step was repeated three times.

2.5.9 Generation of fluorescent fructan polysaccharides

To generate fluorescently labelled inulin and acid-hydrolyzed levan FLA-PS, a previously defined protocol was used [84, 86, 123] with slight modifications. Briefly, 350 µL 0.81 M cyanogen bromide (CNBr; 97%; Sigma C91492) was used to chemically activate 2 mL of 2% carbohydrate sample. Solution was mixed for 5 – 7 min while the pH was closely monitored and maintained above 9.5 with 20 µL additions of 0.25 M NaOH.

The solution was filtered (0.2 μm) and loaded onto an ÄKTA start chromatography system attached to a 29 x 1 cm column containing Sephadex® G-50 gel filtration medium (flow rate: 1 mL min^{-1}) to separate activated carbohydrate from excess CNBr. The mobile phase was 0.2 M sodium tetraborate decahydrate pH 8.0 (≥99.5%; Sigma S9640) . The UV baseline was monitored using Unicorn™ version 2.0 software. The UV peak corresponding to activated carbohydrate was eluted into a vial containing 2 mg fluoresceinamine isomer II (FLA; ~95%; Sigma 07985) which was wrapped in aluminum foil and incubated for ~24 h at room temperature. Excess FLA was removed from the reaction mixture by centrifugation (3 000 *x g*) using Sartorius Vivaspin 15R columns (5 000 MWCO; VS15RH11). Columns were periodically topped off with distilled water during centrifuge cycles until a clear filtrate was obtained. Purified FLA-inulin and FLA-levan were lyophilized in an aluminum wrapped tube and stably stored at -20 °C until further use.

To produce fluorescently labelled fructan oligosaccharides (DP ≤ 20), 1 mL of 2% fructans from barely kernel or stem fraction was activated with 350 μL 0.81 M CNBr. The pH was maintained above 9.5 for 5 – 7 min with 20 μL additions of 0.25 M NaOH. ~6 mg of FLA was directly added to the activated fructans, and solution vial was wrapped in aluminum foil before being incubated at 37 °C for 2 h. 10 mL of 95% ethanol was added to precipitate out FLA-BS and FLA-BK, and a miniature benchtop centrifuge was used to remove excess CNBr and FLA (2 000 *x g,* 5 min). Samples were washed thoroughly with 95% ethanol before being resuspended in ~3 mL distilled water. Solutions were loaded onto a Supelclean™ ENVI-Carb™ SPE tube (3 mL, 250 mg bed wt, Sigma 57088) that was previously conditioned with 2 CV 95% ethanol and equilibrated

with 2 CV distilled water. 3-4 CV 30% ethanol was used to elute off FLA-BS and FLA-BK from the SPE columns. Samples were dried using a sample concentrator (35 °C) before being resuspended in distilled water and lyophilized in an aluminum wrapped tube.

2.5.10 Visualization of FLA-PS uptake with *Bifidobacterium* and *Lactobacillus* species in pure cultures

B. boum, B. merycicum, B. ruminantium, B. globosum were cultured in TPY medium, whereas *L. vitulinus* and *L. ruminis* were cultured in MRS medium. All incubations were performed in an anaerobic chamber (atmosphere: 85% N_2, 10% CO_2, 5% H_2) at 37 °C overnight. The overnight cultures (OD_{600nm} 1.0 – 1.3) were centrifuged at 4 000 *x g*, 10 min and washed two times with 2X carb-free TPY or MRS media. The resulting pellets were resuspended in 2 mL carb-free TPY or MRS media supplemented with 0.5% inulin or 0.5% levan for the FLA-inulin and FLA-levan, respectively. After ~ 24 h of incubation, cultures were centrifuged (5 000 *x g*, 10 min), washed twice with 2X carb-free TPY or MRS media, and resuspended in 2 mL 2X carb-free TPY or MRS media. 20 μL of the 2X carb-free TPY or MRS resuspension was used as the 0 h control, as the cells were not exposed to the FLA-PS. 40 μL aliquots of each sample were taken and combined with 40 μL of 0.4% FLA-inulin or 0.4% FLA-levan, where 20 μL was taken at the 1 d time point. For the FLA-BK and FLA-BS incubations, the *Bifidobacterium* and *Lactobacillus* cells were grown in rich media and were not exposed to 0.5% purified fructans from barley kernel and stem fractions before FLA-PS exposure.

1 mL of 2% formaldehyde (Sigma F8775) was added to each sample and they were incubated overnight at 4 °C. Fixed samples were centrifuged at 5 000 *x g*, 10 min, washed twice with 1X phosphate buffered saline (PBS, pH 7.4), and then resuspended in

1 mL PBS and stored at 4 °C. Samples were diluted and filtered onto a 25 mm (0.2 μm pore size) Isopore™ membrane filter (Sigma GTTP02500), using a 0.45 μm Whatman® cellulose acetate support filter (Sigma WHA10404006) and a gentle vacuum of <200 mbar. Dried filter pieces were counter stained with 4',6-diamidino-2-phenylindole (DAPI) before being mounted onto a glass slide using a 4:1 mixture of Citifluor™ AFI mountant solution (Citifluor 7970-25) to Vectashield® vibrance antifade mounting medium (MJS BioLynx VECTH17002).

2.5.11 Epifluorescence imaging

All samples were visualized using a Leica DM RBE microscope with a cooled 2.8 megapixel camera (Leica DFC 7000T) and a X-Cite 110 LED illumination system with a filter cube containing 365 nm for DAPI and 475 nm for FITC.

2.5.12 Bioinformatic analysis

Assembled genomes (with the RefSeq assembly accession no. in parentheses) of: *B. boum* (GCF_012844085.1), *B. merycicum* (GCF_900129045.1), *B. ruminantium* (GCF_000687635.1), *B. pseudolongum* ssp. *Globosum* (GCF_000800475.2), *L. ruminis* (GCF_000224985.1), and *L. vitulinus* (GCF_000702065.1) were downloaded from the NCBI assembly database. Whole-genome sequences were run through the dbCAN2 meta server [57, 115] HMMscan to determine total CAZyme content (*i.e.,* CAZome) of each species. Predicted CAZyme genes for enzymes belonging to the GH32 family were selected and analyzed by the in-house bioinformatics pipeline, SACCHARIS [56] to determine the phylogenetic relatedness of each specie to each other and GH32 sequences that have been biochemically characterized. Sequences and accession numbers of

characterized GH32 enzymes were extracted from the CAZy database [53, 55], whereby all protein sequences were aligned using MUSCLE [119]. ProtTest3 [134] was used for best-fit model selection, and the phylogenetic tree was created using FastTree [135]. Annotation of the GH32 phylogenetic tree was done in R (version 4.2.0) and Rstudio (version 2022.02.3; Build 492) using the packages ggplot2 [136] , ggtree [137], plyr [138], and treeio [139]. InterProScan [118] and dbCAN2 [57, 58] were used to identify the domain boundaries of each GH32 enzyme.

Chapter 3

Evaluating the prebiotic potential of inulin using metagenomic and metabolic analyses on naïve and inulin-adapted rumen microbial communities

3.1 Introduction

The production of enteric methane (CH_4) resulting from feed digestion by domesticated ruminants, accounts for 17 – 37% of global anthropogenic methane emissions [140, 141]. Additionally, beef and dairy cattle husbandry results in the production of other potent greenhouse gases, such as carbon dioxide (CO_2) and nitrous oxide (N_2O) [142, 143]. Despite these negative environmental impacts, beef production provides several important benefits. For example, on-pasture cattle promote grassland ecosystem biodiversity [144, 145]. Cattle are also unparalleled in their ability to convert plant fibre into meat and dairy products [7]. In comparison, 80% of the diet of other livestock species, such as swine and poultry, is comprised of grains that can digested by humans. For cattle, this requirement is minimal (~5%) and occurs during the finish stage [146]. To minimize the negative environmental impacts of beef production, certain strategies are being explored. Terry *et al*. [7] conducted an comparison of growth-promoting technologies, such as improving the functional efficiency of the rumen microbiome, feed composition, and operational and breeding management practices. The significance improving the production efficiency of beef cattle is underpinned by the growing demand for beef products that is expected to increase by 1.2% per annum until 2050 [2].

Host-microbiome interactions are essential for digestion and overall health of beef cattle [7]. The composition of the rumen microbiome is influenced by a variety of factors including diet [13], physical and genetic differences within the host [147, 148], and feed

additives, such as: antimicrobials [149], probiotics [150, 151], prebiotics [19], and non-nutritive supplements (*e.g.,* essential oils, tannins, saponins) [152, 153]. Diet is the major factor shaping rumen microbiome richness and composition [13], and numerous studies have reported rumen microbiome states are altered between cattle fed fiber-rich diets (*e.g.,* alfalfa, ryegrass) and diets high in rapidly fermentable carbohydrates (*e.g.,* wheat and barley grain) [13, 154-156]. Dietary complex carbohydrates that are selectively utilized by beneficial microbial species within the rumen can result in improved VFA production [19], microbial diversity [157], and feed efficiency [158], with a reduction in enteric methane emissions [159] and the prevention of metabolic disease states, including ruminal acidosis [160] and ketosis [161].

A prebiotic is defined as "a substrate that is selectively utilized by microorganisms conferring a health benefit for the host" [63]. Inulin, a fructose-based polysaccharide containing β-2,1 glycosidic linkages, has been extensively studied for its prebiotic effects in humans and monogastric animals including poultry, swine, canine, and pre-ruminant calves [87]. Inulin fermentation occurs within the large intestine of monogastric animals, where it is selectively utilized by beneficial Bifidobacteria and Lactobacilli resulting in the production of VFAs, lactate, and gas [162]. The combination of antimicrobial substances produced by these beneficial bacteria and the lowered luminal pH resulting from increased VFA production, can lead to the competitive exclusion of pathogens such as *Escherichia coli*, *Campylobacter* spp., and *Salmonella* spp. [80]. Additionally, there have been multiple studies assessing the effect of inulin on enhancing the intestinal mucosal barrier in several animal models [163, 164]. Studies on the prebiotic effect of inulin in ruminants are limited. While the impact of inulin on lactation in dairy cows has

been one focus [165, 166], its potential use for beef cattle has yet to be rigorously investigated. In Chapter 2, I investigated the metabolism of structurally distinct fructans by probiotic bacteria in pure cultures. Here I have expanded this analysis to study how fructans are metabolized in complex rumen communities from cattle fed a commercial source of inulin (Orafti® IPS inulin, BENEO GmbH; Mannheim, Germany) to determine its impact on the composition and metabolic output of naïve and inulin-adapted rumen microbial communities.

3.2 Results

3.2.1 Impact of inulin on artificial rumen systems seeded with naïve microbial communities

3.2.1.1 Volatile fatty acid production

The enrichment of rumen samples with 1.5% and 3% inulin resulted in an increased VFA production over time, where the highest concentration for total VFA production was seen with 3% inulin (204.4 ± 11.4 mM at 48 h; Figure 3.1A). However, individual VFA trends were not consistent between the two inulin concentrations tested. The rumen sample containing 1.5% inulin showed a higher proportion of propionic (19.3 ± 0.2% at 48 h; Figure 3.1C) and butyric (12.9 ± 0.5% at 48 h; Figure 3.1D) acid being produced; whereas, when the inulin concentration was increased to 3%, the production of acetic acid was more abundant (75.1 ± 0.3% at 48 h; Figure 3.1B). In contrast to the main three VFAs produced, the production of other VFAs (*i.e.,* caprioic acid, valeric acid, isovaleric acid, and isobutyric acid; Figure 3.1E) was highest within the control sample, suggesting inulin may reduce their production.

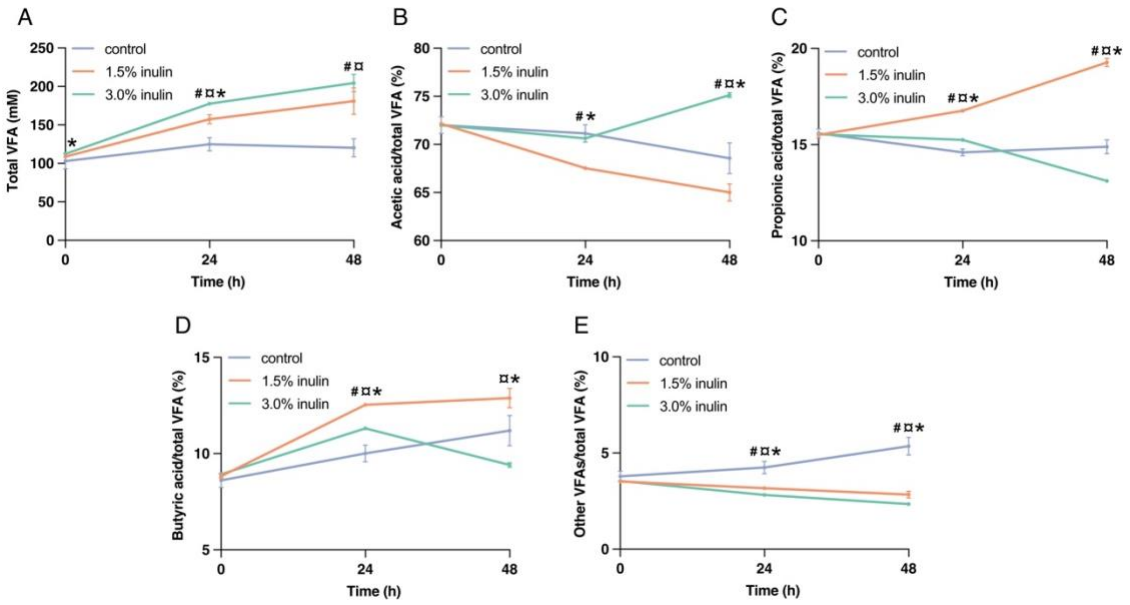

Figure 3.1: Production of volatile fatty acids (VFAs) in artificial rumen systems seeded with naïve microbial communities. (A) Concentration of total VFAs produced and individually VFAs: **(B)** acetic acid, **(C)** propionic acid, **(D)** butyric acid, and **(E)** other VFAs plotted as a percentage of the total, from rumen samples enriched with 1.5% inulin (orange), and 3% inulin (teal), or the negative control (purple). Statistical analysis was performed using multiple t tests where * signifies statistical difference ($p < 0.05$) between 1.5% inulin and 3% inulin treatments. # signifies statistical difference ($p < 0.05$) between 1.5% inulin and control treatments. ¤ signifies statistical difference ($p < 0.05$) between the control and 3% inulin treatments. ($n = 4$).

3.2.1.2 Community analysis

The composition of the rumen microbial communities significantly changed between time points (R = 0.57, p = 0.001; Figure 3.2A) and treatment conditions (R = 0.25, p = 0.002; Figure 3.2B). While the community was predominantly Bacteroidetes (~65%), inulin inclusion increased the abundance of Firmicutes, Actinobacteria, and Euryarchaeota members, particularly at 48 h (Figure 3.2C). The two inulin concentrations had different effects on community structure. An enrichment with 1.5% inulin showed a small increase in community richness; however, 3% inulin resulted in a decreased richness overall (Figure 3.2D). There was a constellation of effects seen when assessing individual taxonomic groups, specifically those with a minimum abundance of 1%. For instance, within inulin-enriched samples there was an increased abundance of Prevotellaceae members seen at 24 h, but this family decreased in abundance at 48 h (Figure 3.3A). There was also a dose-dependent and temporal related increase of beneficial *Bifidobacterium* members seen in response to inulin (Figure 3.3B). A similar relationship was also observed for *Lactobacillus* and other members of the Lactobacillaceae family (*e.g., Limosilactobacillus, Ligilactobacillus*) (Figure 3.3C and 3.3D).

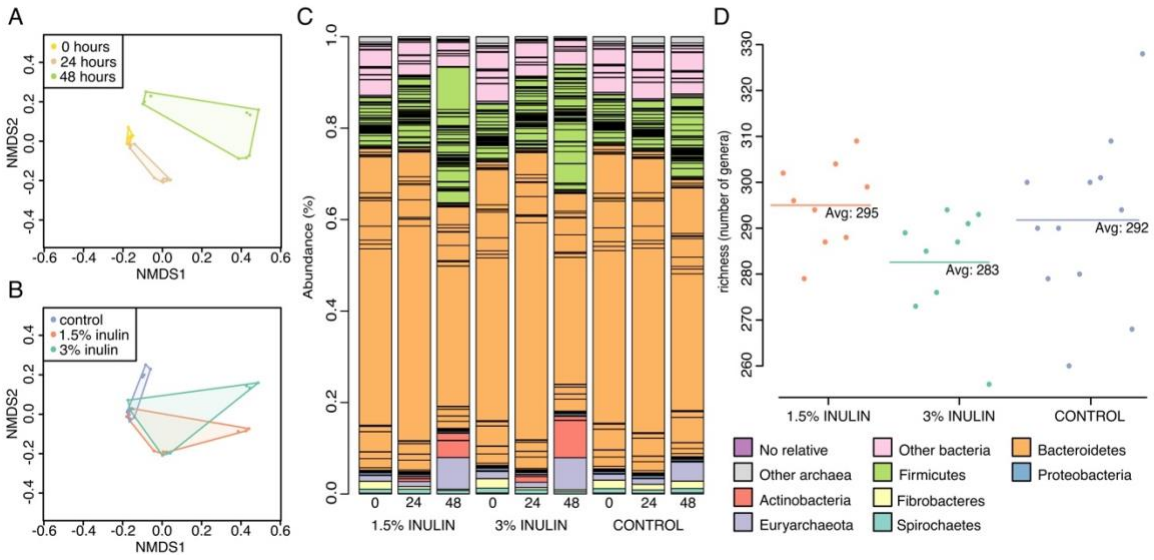

Figure 3.2: Community analysis of artificial rumen systems seeded with naïve microbial communities. (A) Non-metric Multi-dimensional Scaling (NMDS) plot comparing the rumen microbial community composition at different time points: 0 h (yellow), 24 h (beige), and 48 h (green). **(B)** NMDS plot comparing the effect inulin enrichment has on the rumen microbial community composition for control (purple), 1.5% inulin (orange), and 3% inulin (teal). **(C)** Abundance of common ruminal bacterial and archaeal phyla in rumen samples enriched with inulin over 48 h, for samples taken at 0 h, 24 h, and 48 h. **(D)** Richness plot showing the alpha diversity of each enrichment condition by the number of genera present.

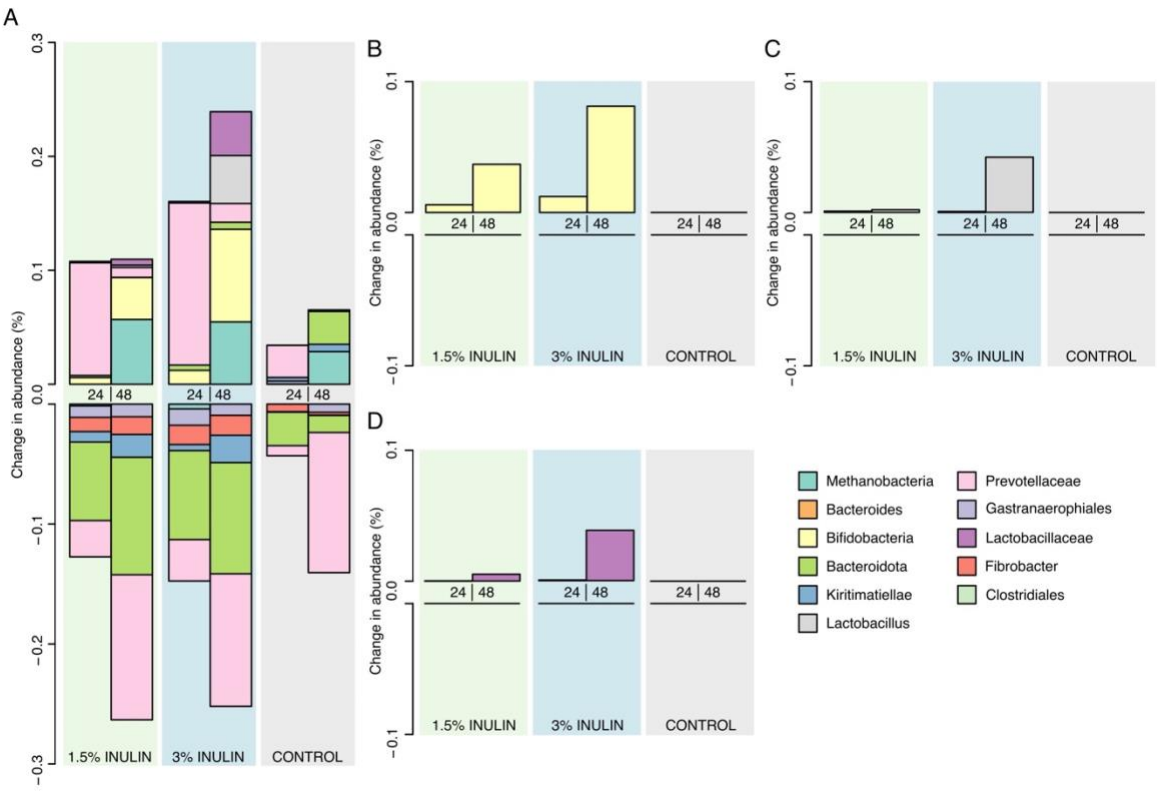

Figure 3.3: Abundance of taxonomic groups in artificial rumen systems seeded with naïve microbial communities. (A) Stacked bar plot of rumen-relevant taxonomic groups that had a minimum abundance of 0.1% relative to their initial abundance. Individual plots of **(B)** *Bifidobacterium* spp., **(C)** *Lactobacillus* spp., and **(D)** other Lactobacillaceae members. Enrichment conditions shown in green (1.5% inulin), blue (3% inulin), and grey (control), and sample time point (24 h, 48 h) shown on the x-axis.

3.2.1.3 Visualization and identification of inulin-metabolizing microbiota

The ability of rumen microbiota to metabolize inulin was assessed using FLA-inulin in control, 1.5% and 3% inulin-enriched conditions. To determine if pre-exposure to inulin increased FLA-inulin uptake, samples were incubated with inulin for 0, h 24 h, and 48 h before being incubated with 0.2% FLA-inulin. Total cell density was determined by enumerating DAPI-stained cells where on average, 20.7% of cells showed uptake of FLA-inulin. Samples that were previously incubated with inulin displayed a dose-dependent increase in FLA-inulin uptake levels (control: 19.1% of $7.7 \times 10^5 \pm 3.9 \times 10^4$ cells mL^{-1}, 1.5% inulin: 19.6% of $8.7 \times 10^5 \pm 4.3 \times 10^4$ cells mL^{-1}, 3% inulin: 23.3% of $9.1 \times 10^5 \pm 3.8 \times 10^4$ cells
mL^{-1}; Figure 3.4).

To investigate correlated taxonomic relationships with inulin, rumen communities were simultaneously incubated with FLA-inulin and either Bif228 or Lacto722 FISH probes [167, 168]. This analysis determined $1.7 \pm 0.3\%$ and $9.3 \pm 1.4\%$ of the initial rumen bacterial communities were identified as *Bifidobacterium* spp. and *Lactobacillus* spp., respectively. An increase in *Bifidobacterium* abundance occurred within the first 24 h of inulin incubation (1.5% inulin: $1.5 \pm 0.2\%$ to $5.1 \pm 3.3\%$; 3.0% inulin: $1.7 \pm 0.3\%$ to $5.6 \pm 3.8\%$). Within the control sample, a smaller increase in *Bifidobacterium* abundance was seen, but this was delayed until 48 h ($1.9 \pm 0.3\%$ to $3.0 \pm 0.6\%$). Of the cells that stained positive with the Bif228 FISH, $0.9 \pm 0.3\%$ of the 3% inulin-enriched community were determined to interact with inulin. This was a small increase from the control and 1.5% inulin samples as these had comparable FLA-inulin utilizing *Bifidobacterium* population proportions (control: $0.7 \pm 0.5\%$, 1.5% inulin: $0.5 \pm 0.7\%$). In comparison,

Lactobacillus spp. were more prevalent within all samples; however, there was no significant change in abundance as the population stayed ~8 – 9% regardless of the sampling time point and treatment condition. A large proportion of *Lactobacillus* spp. showed uptake of FLA-inulin (control: 2.9 ± 1.7%, 1.5% inulin: 2.1 ± 2.0%, 3% inulin: 1.7 ± 1.5%), relative to *Bifidobacterium* members.

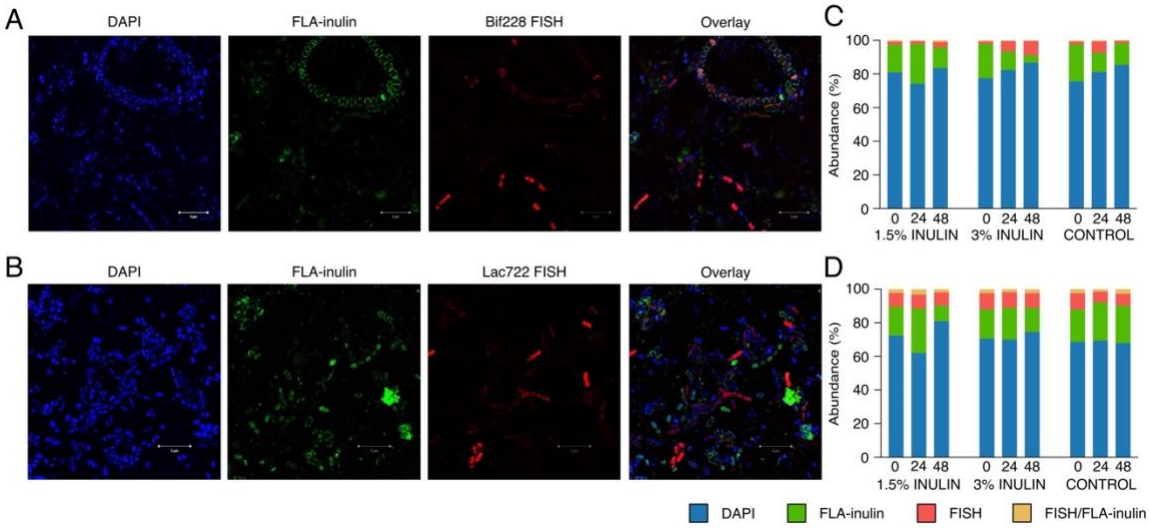

Figure 3.4: Super-resolution (SR-SIM) visualization of FLA-inulin interactions in artificial rumen systems seeded with naïve microbial communities. (A) *Bifidobacterium* spp. identified using Bif228 FISH probe and **(B)** *Lactobacillus* spp. identified using Lac772 FISH probe, and their interaction with FLA-inulin in a 3% inulin enriched rumen sample taken after 48 h, and subsequently incubated with 0.2% FLA-inulin for 24 h. DAPI used to stain DNA and the SR-SIM scale indicates a length of 5 µm. **(C)** Enumeration of microbial samples incubated with FLA-inulin and the Bif228 FISH probe. **(D)** Enumeration of microbial samples incubated with FLA-inulin and the Lac722 FISH probe.

3.2.2 Impact of inulin on artificial rumen systems seeded with inulin-adapted microbial communities

3.2.2.1 Production of volatile fatty acids, ammonia, and gas

No significant effect on total VFA production (Figure 3.5A) or individual VFA profiles (Supplementary Figure 2) was seen when rumen samples extracted from cattle fed an inulin-enriched diet were analyzed. In addition, ammonia production was not significantly altered (Figure 3.5B). Upon closer examination, half of the biological samples displayed decreased production of ammonia (Supplementary Figure 3). In contrast, samples taken from inulin-adapted rumen systems, resulted in a significant decrease in total gas production during the length of the experiment (Figure 3.5C).

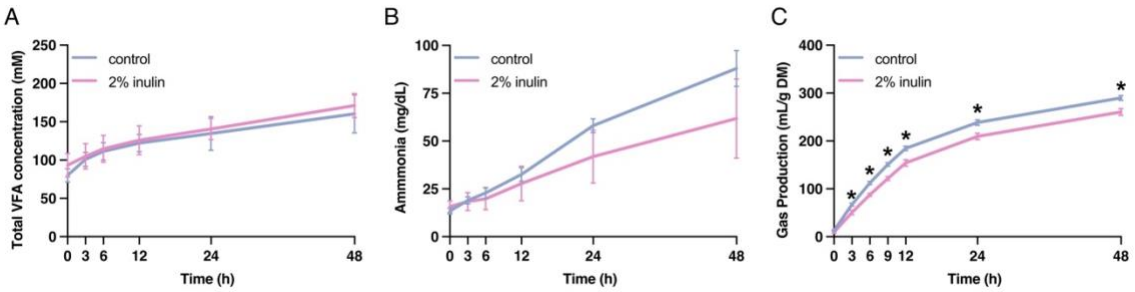

Figure 3.5: Metabolic outputs of artificial rumen systems seeded with inulin-adapted microbial communities. Cattle were fed basal or 2% inulin supplemented diets for 17 d prior to sampling. *In vitro* measurements were conducted, where **(A)** total VFA, **(B)** ammonia, and **(C)** total gas production were measured at 0 h, 3 h, 6 h, 9 h (gas only), 12 h, 24 h, and 48 h. (n = 4 biological replicates per treatment). Statistical analysis was performed using multiple t tests where * signifies statistical difference ($p < 0.05$) between control and 2% inulin supplemented rumen samples.

3.2.2.2 Community analysis

The composition of rumen microbial communities significantly changed between time points (R = 0.763, p = 0.001; Figure 3.6A), but not in response to the treatment condition (R = 0.076, p = 0.169; Figure 3.6B). On average, the community richness was higher within inulin-adapted rumen samples (Figure 3.6C). Bacteroidetes within these communities were not as prevalent (~45%) compared to the naïve samples previously examined (Figure 3.2C); notably, Firmicutes, Euryarchaeota, and other bacterial phyla increased over time (Figure 3.6E). Looking at individual taxa that accounted for some of these compositional changes, the Clostridia UCG-014 order, Ruminococcaceae *CAG-352* and Succinivibrionaceae *UCG-002* genera showed increased abundance in 2% inulin-adapted communities (Figure 3.6F). *Bifidobacterium* spp. and *Lactobacillus* spp. remained relatively low in both conditions, where *Bifidobacterium* spp. increased to a greater extent within the inulin-adapted community over time (Figure 3.6D). In contrast, the abundance of *Lactobacillus* and other Lactobacillaceae were almost negligible; yet a small increase was seen over time within the inulin-adapted samples (Figure 3.6D).

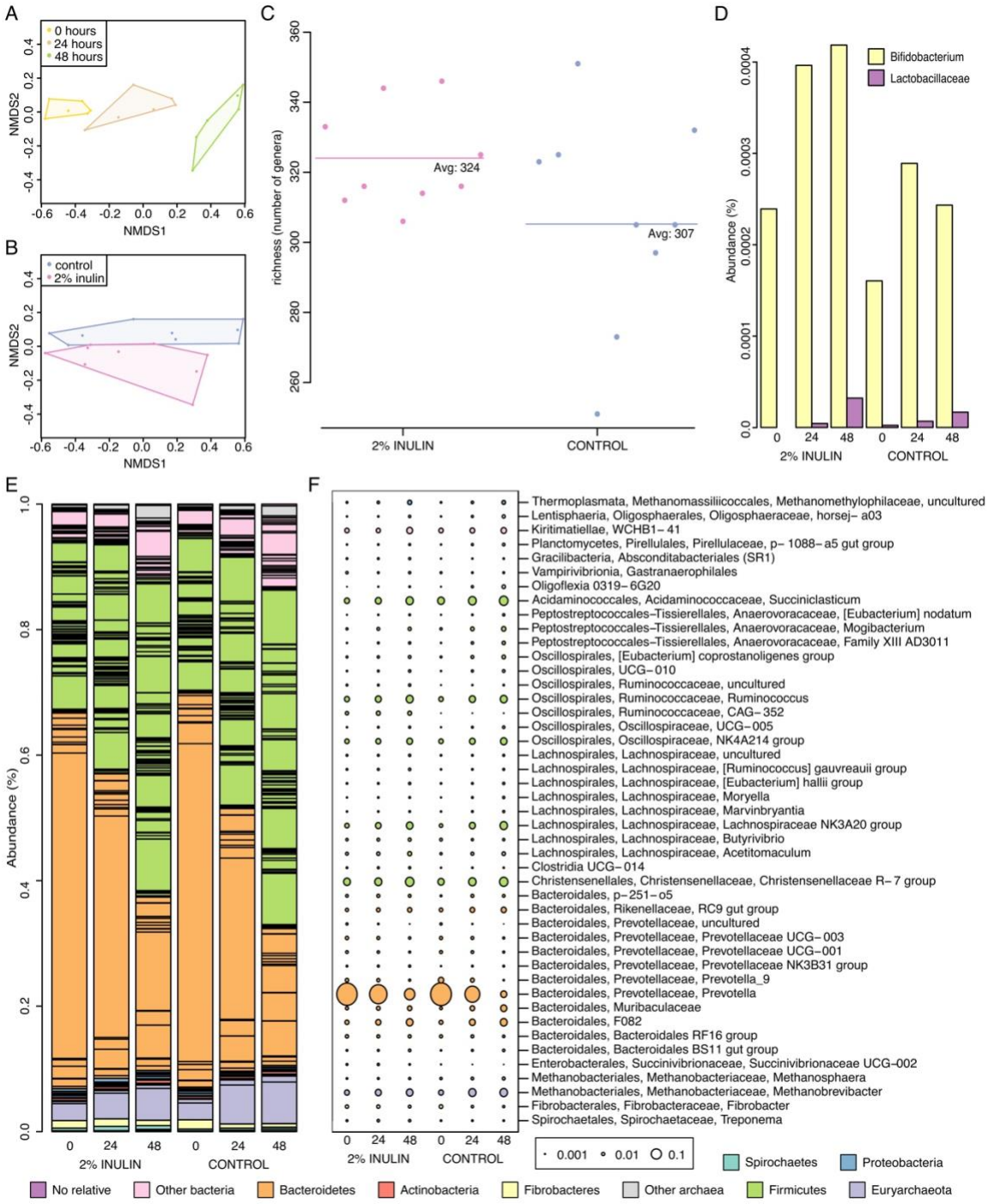
A
0 hours
24 hours
48 hours
NMDS2
NMDS1
B
control
2% inulin
NMDS2
NMDS1
C
richness (number of genera)
Avg: 324
Avg: 307
2% INULIN
CONTROL
D
Bifidobacterium
Lactobacillaceae
Abundance (%)
0 24 48 0 24 48
2% INULIN
CONTROL
E
Abundance (%)
0 24 48 0 24 48
2% INULIN
CONTROL
F
Thermoplasmata, Methanomassiliicoccales, Methanomethylophilaceae, uncultured
Lentisphaeria, Oligosphaerales, Oligosphaeraceae, horsej– a03
Kiritimatiellae, WCHB1– 41
Planctomycetes, Pirellulales, Pirellulaceae, p– 1088– a5 gut group
Gracilibacteria, Absconditabacteriales (SR1)
Vampirivibrionia, Gastranaerophilales
Oligoflexia 0319– 6G20
Acidaminococcales, Acidaminococcaceae, Succiniclasticum
Peptostreptococcales–Tissierellales, Anaerovoracaceae, [Eubacterium] nodatum
Peptostreptococcales–Tissierellales, Anaerovoracaceae, Mogibacterium
Peptostreptococcales–Tissierellales, Anaerovoracaceae, Family XIII AD3011
Oscillospirales, [Eubacterium] coprostanoligenes group
Oscillospirales, UCG– 010
Oscillospirales, Ruminococcaceae, uncultured
Oscillospirales, Ruminococcaceae, Ruminococcus
Oscillospirales, Ruminococcaceae, CAG– 352
Oscillospirales, Oscillospiraceae, UCG– 005
Oscillospirales, Oscillospiraceae, NK4A214 group
Lachnospirales, Lachnospiraceae, uncultured
Lachnospirales, Lachnospiraceae, [Ruminococcus] gauvreauii group
Lachnospirales, Lachnospiraceae, [Eubacterium] hallii group
Lachnospirales, Lachnospiraceae, Moryella
Lachnospirales, Lachnospiraceae, Marvinbryantia
Lachnospirales, Lachnospiraceae, Lachnospiraceae NK3A20 group
Lachnospirales, Lachnospiraceae, Butyrivibrio
Lachnospirales, Lachnospiraceae, Acetitomaculum
Clostridia UCG– 014
Christensenellales, Christensenellaceae, Christensenellaceae R– 7 group
Bacteroidales, p– 251– o5
Bacteroidales, Rikenellaceae, RC9 gut group
Bacteroidales, Prevotellaceae, uncultured
Bacteroidales, Prevotellaceae, Prevotellaceae UCG– 003
Bacteroidales, Prevotellaceae, Prevotellaceae UCG– 001
Bacteroidales, Prevotellaceae, Prevotellaceae NK3B31 group
Bacteroidales, Prevotellaceae, Prevotella_9
Bacteroidales, Prevotellaceae, Prevotella
Bacteroidales, Muribaculaceae
Bacteroidales, F082
Bacteroidales, Bacteroidales RF16 group
Bacteroidales, Bacteroidales BS11 gut group
Enterobacterales, Succinivibrionaceae, Succinivibrionaceae UCG–002
Methanobacteriales, Methanobacteriaceae, Methanosphaera
Methanobacteriales, Methanobacteriaceae, Methanobrevibacter
Fibrobacterales, Fibrobacteraceae, Fibrobacter
Spirochaetales, Spirochaetaceae, Treponema
0 24 48 0 24 48
2% INULIN
CONTROL
0.001 0.01 0.1
Spirochaetes
Proteobacteria
No relative
Other bacteria
Bacteroidetes
Actinobacteria
Fibrobacteres
Other archaea
Firmicutes
Euryarchaeota

Figure 3.6: Community analysis of artificial rumen systems seeded with inulin-adapted microbial communities. (A) NMDS plot comparing the rumen microbial community composition at different time points: 0 h (yellow), 24 h (beige), and 48 h (green). **(B)** NMDS plot comparing the effect inulin-adaptation has on the rumen microbial community composition, control (purple) and 2% inulin-adapted (pink). **(C)** Richness plot showing the alpha diversity of control (purple) and 2% inulin-adapted (pink) rumen samples. The abundance of *Bifidobacterium* spp. and Lactobacillaceae species., and **(D)** common ruminal bacterial and archaeal phyla **(E)** in naïve and inulin-adapted rumen samples assessed over 48 hours. **(F)** Most abundant taxonomic groups and their abundance trends in inulin-adapted rumen samples over 48 hours, with the order, family, and genus level shown.

3.2.2.3 Visualization of FLA-inulin utilization

A lower FLA-inulin concentration of 0.02% was used to assess inulin utilization within inulin-adapted rumen samples. This concentration was deemed too low for automatic cell enumeration; but uptake was still be assessed by manual cell counting. FLA-inulin uptake was measured at 5 min, 1 h, and 24 h time points to determine if there was a temporal difference between samples ± inulin-adaptation. FLA-inulin utilization was observed in both rumen communities; however, there was a larger response seen in the inulin-adapted samples that occurred at both the 1 h and 24 h time points (Figure 3.7). The use of Bif228 and Lacto722 FISH probes highlighted a subset of cells within the control samples that were detectable within the 5 m time point, showing an increased abundance after 24 h of incubation with FLA-inulin. Whereas, within the inulin-adapted samples, an increase in *Lactobacillus* spp. occurred at 5 min and at 1 h for *Bifidobacterium* spp. (Figure 3.7).

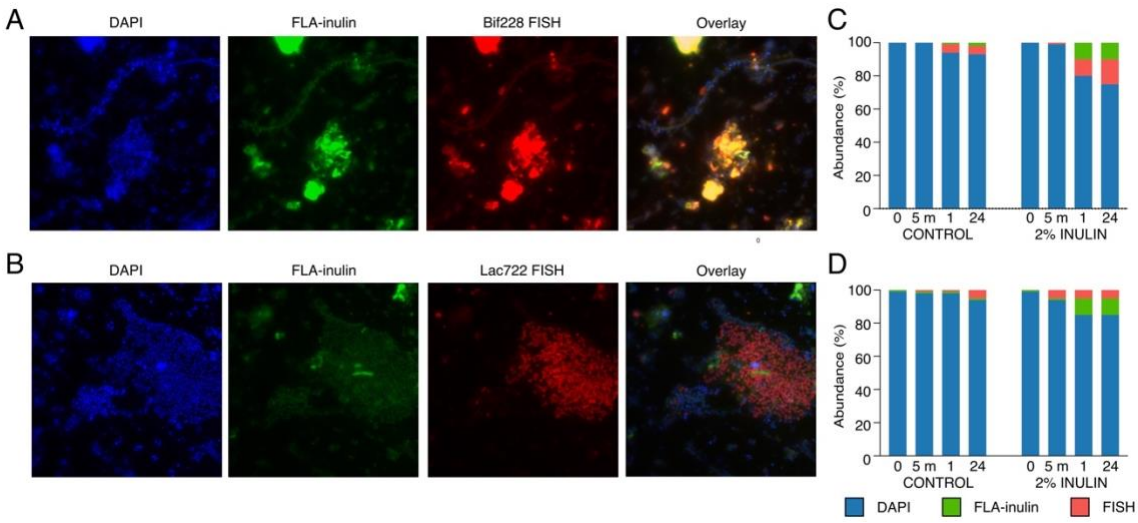

Figure 3.7: Epifluorescence visualization of FLA-inulin interactions in artificial rumen systems seeded with inulin-adapted microbial communities. (A) *Bifidobacterium* spp. identified using Bif228 FISH probe and **(B)** *Lactobacillus* spp. identified using Lac772 FISH probe, and their interaction with FLA-inulin in inulin-adapted rumen sample, where samples were incubated with 0.2% FLA-inulin for 24 h. DAPI used to stain DNA. **(C)** Estimated enumeration of microbial samples incubated with FLA-inulin and the Bif228 FISH probe. **(D)** Estimated enumeration of microbial samples incubated with FLA-inulin and the Lac722 FISH probe.

3.3 Discussion

The production of VFAs are essential to overall animal performance and can supply up to 70% of the host's energy needs [169]. Besides serving as an energy substrate, chemically distinct VFAs differ in their roles regulating physiological functions of the rumen. For instance, butyric acid is known for stimulating and regulating the growth and function of the ruminal epithelium [170, 171], whereas propionic acid is used within the liver for gluconeogenesis [172]. The diet composition (*e.g.,* forage:concentrate ratio) can affect the proportions individual VFAs are produced in. Indeed, the enrichment of naïve rumen samples with inulin had significant effects on *in vitro* VFA production, where 1.5% inulin resulted in propionic and butyric acid being favoured, and the production of acetic acid was dominant within the 3% inulin enriched samples (Figure 3.1). These results are in agreement with the current state of literature regarding the effect of inulin on ruminal VFA production; other *in vitro* rumen studies found that the production of propionic and butyric acid was favoured within samples enriched with 2% inulin [173, 174]. Additionally, Tian *et al.* [72] discovered that an inclusion of 2% inulin in a low concentrate diet (40% concentrate) fed to finishing beef cattle resulted in increased propionic, butyric, and isobutryic concentrations, however when inulin was supplementation into a high concentrate diet (60%), no significant effects on VFA production were found. Within this study, rumen microbial communities adapted to a high forage diet (50% alfalfa hay, 35% barley silage) with 2% inulin did not result in a significant change in VFA production. Differences in the results of the experiments carried out within this paper, suggest that inulin has limited prebiotic potential within the rumen microbiome, as it does not result in long-term effects on VFA production, with respect to high forage diets. While initial effects were seen in rumen samples taken from

cattle fed a 50:50 forage:concentrate diet, long term effects will need to be studied using this diet formulation to see the impact forage:concentrate ratios have on dietary inulin.

The rumen microbiome is highly efficient in converting host-indigestible plant fiber [175]; therefore, it is unclear if prebiotics such as inulin, will have a substantial effect within this ecosystem [66]. Data presented here showed that 19.1% of the rumen microbial community was able to utilize inulin without previous exposure (Figure 3.4). This suggests that inulin-utilizing bacteria are indigenous in the rumen in high numbers, perhaps resulting from the presence of fructans in conventional diets [39, 176]; however, this was not determined. Responses to inulin could be improved. Exposure to 3% inulin for 48 h resulted in a 4.2% increase in cells that interact with inulin (Figure 3.4). When compared to other prebiotics, Klassen *et al.* [86] discovered that 6.1 ± 0.5% of the rumen community utilized YM, where nearly half of these YM-metabolizing members were identified as Bacteroidetes. Addition of Bio-Mos®, a commercial prebiotic containing YM, resulted in an increase to 7.7% of the rumen microbial community being identified as YM consumers [177]. Notably, the structure of these two prebiotics differ as inulin contains 1 terminal glucose and ≤ 60 fructosyl residues connected by β-2,1 glycosidic linkages [34]; whereas YM is more complex containing 4 different linkages (*i.e.,* α-1,2; α-1,3; α-1,6; and β-1,4) between mannose, and N-acetylglucosamsyl and phosphate residues [178]. While YM catabolism requires several GHs (*i.e.,* GH99, GH76, GH92, GH38, GH125), the breakdown of inulin is more straightforward, as in most cases only a single GH32 enzyme is required ([62, 178]; see Chapter 2). Therefore, the increased proportion of the rumen microbial community that was able to utilize inulin versus YM

[86, 177] is reasonable as previous exposure to less structurally complex prebiotics would be consumed within the rumen more easily.

Dietary inulin is known to be a prebiotic for *Bifidobacterium* spp. and *Lactobacillus* spp. [109, 162, 179, 180], which is associated with improved health and well-being of the host [181, 182]. The addition of inulin to naïve rumen samples resulted in an increased abundance of *Bifidobacterium* spp., *Lactobacillus* spp., and other lactic acid bacteria; this increase occurred in a dose-dependent manner (Figures 3.3 and 3.4). This result is in agreement with what has been reported in monogastric animals. Inulin was a prebiotic for lactic acid bacteria and other beneficial bacteria (*e.g., Muribaculaceae*) when supplemented at various supplementation concentrations (1 – 4%) in swine, poultry, and other animals [110, 183-185]. Closer examination of inulin consuming bacteria within 3% inulin-enriched samples revealed that *Bifidobacterium* spp. and *Lactobacillus* spp. made up 0.9 ± 0.3% and 1.7 ± 1.5% of the community, respectively (Figure 3.4). Of the species that were studied, the observation that the Lactobacilli had a higher propensity to utilize fructans in Chapter 2 could result from possessing more than 1 GH32. Although, inulin utilization by these species was also observed in inulin-adapted rumen samples (Figure 3.7) the overall abundance was drastically lowered within these samples (Figure 3.6D). This suggests that increased dietary fibre or competition with fibre-utilizing bacteria might have impacted the abundance of these genera to a greater extent than the inclusion of 2% inulin.

The addition of inulin to adapted and naïve rumen samples had other impacts on microbial composition. For instance, community richness increased to a small degree when naïve rumen samples were enriched with 1.5% inulin (Figure 3.2D), and to a

greater extent in inulin-adapted communities *ex vivo* (Figure 3.6C). Tian *et al.* [72] found that 2% inulin inclusion in a high concentrate diet (60%) resulted in increased community richness after 42 d. In contrast, a further increase in inulin enrichment seems to decrease microbial richness in naïve communities (Figure 3.2D). These results suggest that >2% inulin supplementation may result in lowered community richness. Assessing the impact on taxa other than *Bifidobacterium* spp. and *Lactobacillus* spp., the abundance of *Prevotellaceae* was positively affected within the first 24 h of inulin enrichment; whereas by 48 h, the change in abundance decreased below the abundance observed at 0 h (Figure 3.3A). Within inulin-adapted samples, the abundance of *Prevotellaceae* decreased overtime as an effect of the growth conditions but occurred less drastically within the 2% inulin samples (Figure 3.6F). Similarly, Tian *et al.* [72] found that inulin supplementation decreased the abundance of *Prevotellaceae,* along with *Succinticlasticum* spp. and *ruminiococcus* spp.. This trend may result by an initial abundance of starch and simple carbohydrates, which are consumed during the course of the incubation and are not available as substrates at the 48 h time point.

3.4 Conclusion

The addition of inulin to naïve rumen samples *in vitro* demonstrated that inulin has potential as a prebiotic for beef cattle; however, its potential was moderated when studied in animals that were previously adapted to 2% inulin. Differences between these 2 experiments may explain some of these results, as rumen sample used in the batch culture study were collected from a cow fed a high concentrate diet (50%) without previous exposure to inulin. In contrast, animals used within the feeding trial consumed a high forage diet that contained 50% alfalfa hay and samples were collected 17 days after diet

adaptation. Clearly, diet composition and sampling time (*e.g.,* adaptation phase, post-adaptation) have an effect on the microbial composition on the rumen [13, 186], and should be taken into consideration when assessing other feed additives for prebiotic potential in the future. Moving forward, while the addition of inulin increased the microbial richness within the rumen, it is unclear if the prebiotic quality of enhancing beneficial *Lactobacillus* spp. and *Bifidobacterium* spp. that is seen within monogastric and *in vitro* inulin enrichment of rumen samples, can occur to a significant extent within an animal model.

3.5 Materials and methods

3.5.1 Inulin enrichment in artificial rumen system seeded with naïve rumen microbial communities

3.5.1.1 Sample collection and processing

Rumen sample was collected from a cannulated, non-lactating Angus cow fed a basal diet composed of 50% barley silage, 50% barley grain, with a mineral and vitamin supplement. The rumen sample was filtered through two layers of cheesecloth before being transferred into an anaerobic chamber (atmosphere: 85% N_2, 10% CO_2, 5% H_2, at 37 °C) for *in vitro* batch culture experimentation. The sample was equally distributed into three tubes, where one tube contained 1.5% Orafti® IPS inulin, the second contained 3% Orafti® IPS inulin, and the final tube contained no inulin. The tubes were incubated anaerobically for 48 h with occasional mixing. 5 mL aliquots were taken from each tube at 0, 24, and 48 h time points and were used for downstream 16S metagenomics, VFA analysis, and FLA-inulin/FISH incubations.

From the 5 mL aliquots, 2 mL of each sample was centrifuged (20 000 *x g*, 10 min) and supernatants were removed. DNA from the resulting pellets was extracted using the DNeasy PowerSoil Pro Kit (Qiagen 47016) following manufacturer's instructions. Purified DNA samples were sent to Genome Québec for Illumina MiSeq PE250 16S rRNA metagenomics sequencing using the primers 515F (5' GTGCCAGCMGCCGCGGTAA 3') and 806R (5' GGACTACHVGGGTWTCTAAT 3') to target the V4 region. The BBTools software [187] was used to perform quality trimming and merging of the 16S rRNA sequences. Clustering and classification of the reads were done through the SILVAngs pipeline using the standard settings and the SSU rRNA seed of the SILVA database release 132 [188]. Analyses and plotting of the microbial community data were done using R version 4.2.0 and RStudio version 2022.02.3 (Build 492) using the packages: Phyloseq [189], picante [190], ggplot2 [136], and rioja [191]. Phyla chosen for plotting microbial abundance were chosen based on core rumen microbiome members that were previously reported [192, 193]. Triplicate technical replicates of each sample were used for the metagenomic analysis, there were no significant differences between replicates and for plotting purposes only the average analysis was used.

3.5.1.2 Measurement of volatile fatty acid (VFA) production

For VFA analysis, 1.5 mL of the 5 mL aliquots was directly added to 0.3 ml 25% meta-phosphoric acid (Fisher Scientific A280) on ice. Samples were mixed and stored at -20 °C until gas chromatographic analysis [194, 195]. VFA data was plotted in GraphPad Prism version 9.1.1 and statistically analyzed by multiple t tests.

3.5.1.3 FLA-inulin incubations

1 mL aliquots from the 1.5% inulin, 3% inulin, and control rumen samples were added to 1 mL of 0.4% FLA-inulin and incubated anaerobically at 37 °C. From each sample, aliquots were collected at 0 (prior to FLA-inulin addition), 1, and 24 h time points. Cells were immediately fixed with 2% formaldehyde (FA) at 4 °C overnight. Samples were centrifuged (5 000 *x g*, 10 min) and pellets were washed twice with 1X phosphate buffered saline (PBS) before being resuspended in 1 mL PBS and stored at 4 °C. After cell fixation, samples were diluted and filtered onto a 25 mm (0.2 μm pore size) Isopore™ membrane filter (Sigma GTTP02500), using a 0.45 μm Whatman® cellulose acetate support filter (Sigma WHA10404006) and a gentle vacuum of <200 mbar. Dried filter pieces were used for fluorescence *in vitro* hybridization (FISH) staining.

3.5.1.4 Fluorescence in situ hybridization (FISH) and epifluorescence visualization

For FISH, the oligo-nucleotide probes Bif228 targeting *Bifidobacterium* (5'-GATAGGACGCGACCCCAT-3') [167] and Lacto722 targeting *Lactobacillus* (5'-YCACCGCTACACATGRAGTTCCACT-3') [168] were each covalently labelled with four ATTO590 fluorochromes by Integrated DNA Technologies (Iowa, United States) prior to use. The FISH hybridization buffer contained 900 mM NaCl, 20 mM Tris-HCl (pH 7.5), 0.01% sodium dodecyl sulfate, and a formamide concentration of either 20% or 5% for the Bif228 and the Lacto722 samples respectively. Hybridizations were performed within a 46 °C chamber for 3 h before undergoing a subsequent 15 min wash at 48 °C in a buffer containing 20 mM Tris-HCl (pH 7.5), 2 nM EDTA (pH 8.0), 0.01% sodium dodecyl sulfate, and a NaCl concentration of either 215 mM and 630 mM for the Bif228 and the Lacto722 samples, respectively. After FISH, filter pieces were washed with

distilled H_2O and dried before being counter stained with DAPI and mounted onto a glass slide using a 4:1 mixture of Citifluor™ AFI mountant solution (Citifluor 7970-25) to Vectashield® vibrance antifade mounting medium (MJS BioLynx VECTH17002).

All rumen samples were visualized and enumerated using a fully automated microscope imaging system, as previously described in detail by Bennke et al. [196], on a Zeiss AxioImager Z2 microscope stand (Carl Zeiss MicroImaging GmbH; Göttingen, Germany) with a cooled charged-coupled device (CCD) camera (AxioCam MRm; Carl Zeiss) and a Colibri LED light source (Carl Zeiss) with three light-emitting diodes (UV-emitting LED, 365 ± 4.5 nm for DAPI; blue emitting LED, 470 ± 14 nm for FLA-PS 488; red-emitting LED, 590 ± 17.5 nm for the tyramide Alexa 594, FISH, combined with the HE-62 multifilter module (Carl Zeiss). This module consists of a triple emission filter TBP 425 (±25), 527 (±27), LP 615, including a triple beam splitter of TFT 395/495/610. All automatic cell counts were validated using manual cell counting. After image acquisition the images were imported into the ACMETOOL3.0 image analysis software (https://www.mpi-bremen.de/en/automated-microscopy.html). From the images cells are classified as FISH stained or as showing substrate uptake (FLA-inulin) if they show a positive signal in both the DAPI and FLA-PS (488) or FISH (549) images, respectively. Additionally, these signals must have a minimum overlap of 30% and minimum area of 17-30 pixel and minimum signal to background ratio of 2 [196]. Microbial abundance was plotted in GraphPad Prism version 9.1.1.

3.5.1.5 Super-resolution structured illumination (SR-SIM) imaging

Rumen samples were visualized on a Zeiss ELYRA PS.1 (Carl Zeiss) using 561, 488m and 405 nm lasers and BP 573-613, BP 502-538 and BP 420-480+LP 750 optical

filters. Z-stack images were taken with a Plan-Apochromat 63 Å~ /1.4 Oil objective and processed with the software ZEN2011 (Carl Zeiss).

3.5.2 Inulin enrichment in an artificial rumen system seeded with inulin-adapted microbial communities

3.5.2.1 Experimental design of feeding trial and sample collection

The Canadian Council of Animal Care guidelines (ACC2107) were followed [197]. Standard husbandry practices were employed throughout the duration of this study. Rumen-cannulated, non-lactating Angus cows were fed a basal diet consisting of 50% alfalfa hay, 35% barley silage, 12% barley grain, and a 3% vitamin and mineral supplement (control) or a 2% Orafti® IPS inulin enriched version of the basal diet (for each diet: $n = 4$), for 20 days. For the first 7 days, the animals were adapted to the diets by gradually increasing the amount of feed in a stepwise manner. For each increase in feed, if the dry matter intake dropped by ≥ 20% (based on the previous 3 days), supplementation rate was no longer increased until the intake rebounded. If no rebound occurred, supplementation rate was decreased.

Biological replicates of rumen samples were collected on day 17, 2 h after feeding ($n = 4$ per treatment). Samples were filtered through two layers of cheesecloth and were pooled by diet condition before being transported into an anaerobic chamber (atmosphere: 85% N_2, 10% CO_2, 5% H_2, at 37 °C). 48 mL aliquots were added into vials containing 500 mg of feed (in accordance with the diets the cattle were already on) ± 2% Orafti® IPS inulin. 7 mL aliquots were taken from samples at 0 h, 3 h, 6 h, 9 h (gas only), 12 h, 24 h, and 48 h time points and used for downstream 16S metagenomics, analysis of VFA and ammonia production, and FLA-inulin/FISH incubations. Separate vials were used to

measure gas production to prevent changes in sample volume from affecting measurements (n = 4 per treatment).

3.5.2.2 Metabolic output measurements

For total gas measurements, a 22G 1½ inch needle was attached to a Fisherbrand™ Traceable™ manometer pressure/vacuum gauge (Fischer Scientific 9002376) was used. For each read, the needle was inserted into the rubber stopper capping each vial. After a stable gas reading was recorded, the vial was vented of any remaining gas by disconnecting the needle from the gauge. Gas data was plotted in GraphPad Prism version 9.1.1 and statistically analyzed by multiple t tests. For VFA analysis, 1.5 mL of the 5 mL aliquots was directly added to 0.3 ml 25% meta-phosphoric acid (Fischer Scientific A280) on ice. Samples were mixed and stored at -20 °C until gas chromatography analysis [194, 195]. VFA data was plotted in GraphPad Prism version 9.1.1 and statistically analyzed by multiple t tests. For ammonia analysis, 1.5 mL of sample was added to 0.3 mL 2% sulfuric acid on ice. Samples were mixed and stored at -20 °C until analysis using a segmented flow analyzer [198, 199]. Ammonia data was plotted in GraphPad Prism version 9.1.1 and statistically analyzed by multiple t tests.

3.5.2.3 FLA-inulin incubations

FLA-inulin was prepared as previously described in Section 2.5.9. 1 mL sample aliquots taken on day 15 of the animal trial from cows fed basal and 2% inulin enriched diets, where they were incubated with 1 mL of 0.04% FLA-inulin for 1 day before being fixed and visualised by epifluorescence microscopy. A final FLA-inulin concentration of

0.02% was deemed too low for automatic cell enumeration, therefore cell enumeration counts were done manually.

Chapter 4

Conclusions and future directions

In this project, fructans from the kernels and stems of winter wheat, spring wheat, and barley plants, collected seven days after anthesis, were purified and structurally characterized. A DP range of 3 – 12 was observed for each cereal crop fraction, and graminan-type (mixed-linkage) fructans were observed, based on inferences from previous studies. Confirmation of these structures will require absolute structural determination by NMR or identification of suitable standards. Utilization of purified and commercial fructans was assessed by growth studies and FLA-PS uptake experiments using species of *Bifidobacterium* and *Lactobacillus* isolated from cattle. Each specie was determined to possess at least one GH32 enzyme, which is associated with fructan metabolism. *B. boum*, *B. merycicum*, and *L. vitulinus* showed early uptake of the cereal crop fructans and each species grew on inulin; however, *L. vitulinus* was the only species able to metabolize and interact with levan. This observation is by the presence of a GH32 enzyme with predicted fructan β-fructosidase activity, allowing this specie to potentially cleave terminal fructosyl residues in levan. The prebiotic potential of inulin was further assessed in rumen microbial communities. Inulin increased VFA production and proliferation of Bifidobacteria and Lactobacilli when naïve rumen microbial communities were incubated with inulin for 48 h. When rumen samples were extracted from cannulated cattle adapted to an inulin-enriched diet, the prebiotic effects were not observed, which suggests that inulin has limited prebiotic potential to modulate rumen microbial communities. This project demonstrated that immature cereal crops are sources of fructan prebiotics, and inulin has potential as a prebiotic in ruminants using different fructan types and artificial rumen system methods. Further work will be required to

investigate other inulin-utilizing members in the rumen microbial community, as well as additional work to demonstrate if diverse fructans stimulate of prebiotic, probiotic, and synbiotics effects in cattle in a commercial setting.

4.1 Fluorescence activated cell sorting and sequencing (FACSeq)

An average of 20.7% of the rumen microbial community showed utilization of FLA-inulin without prior inulin-adaptation (Figure 3.4). This suggests that the majority of bacteria (~80%) do not belong to the *Bifidobacterium* and *Lactobacillus* genera. Potentially, these taxa could be sorted and identified using FACSeq. I hypothesize that these sorted communities would contain genes necessary for fructan transport and GH32s, required for fructan depolymerization. If cultivatable, these species may also represent novel sources of probiotics for beef cattle.

4.2 Assessing other fructan types as potential prebiotics for ruminants

The utilization of cereal crop fructans was found to occur rapidly by *Bifidobacterium* and *Lactobacillus* species isolated from cattle; however, it is not known how these bacteria would respond within a complex community, as they would be in competition with other bacteria capable of metabolizing fructans. I hypothesize that the responses of these individual species would be muted *in vivo*; however, in this case, alternative indigenous species would provide similar ecological services and health benefits to host. Other fructan types, such as levan which was only able to be metabolized by *L. vitulinus*, may provide more specificity within the rumen. This relationship could be explored using levan sourced from bluegrass and Poales grasses [36, 100].

References

1. United Nations, D.o.E.a.S.A., Population Division *World Population Prospects 2019: Highlights.* 2019.
2. Alexandratos, N. and J. Bruinsma, *World Agriculture Towards 2030/2050: The 2012 Revision*. 2012: FAO, Agricultural Development Economics Division.
3. CRSB, C.R.T.f.S.B., *National beef sustainability assessment and strategy summary report.* Calgary, AB: CRSB., 2016.
4. BCRC, *Priority area review: Feed grains and feed efficiency.* 2017.
5. Pulina, G., et al., *Animal board invited review – Beef for future: technologies for a sustainable and profitable beef industry.* Animal, 2021. **15**(11): p. 100358.
6. Kenny, D.A., et al., *Invited review: Improving feed efficiency of beef cattle – the current state of the art and future challenges.* Animal, 2018. **12**(9): p. 1815-1826.
7. Terry, S.A., et al., *Strategies to improve the efficiency of beef cattle production.* Canadian Journal of Animal Science, 2020. **101**(1): p. 1-19.
8. Koch, R.M., et al., *Efficiency of Feed Use in Beef Cattle.* Journal of Animal Science, 1963. **22**(2): p. 486-494.
9. Elolimy, A.A., et al., *Residual feed intake in beef cattle and its association with carcass traits, ruminal solid-fraction bacteria, and epithelium gene expression.* Journal of Animal Science and Biotechnology, 2018. **9**(1): p. 67.
10. Paz, H.A., et al., *Rumen bacterial community structure impacts feed efficiency in beef cattle.* Journal of Animal Science, 2018. **96**(3): p. 1045-1058.
11. Abbas, W., et al., *Influence of host genetics in shaping the rumen bacterial community in beef cattle.* Scientific Reports, 2020. **10**(1): p. 15101.
12. Chen, F., et al., *Rumen Microbiota Distribution Analyzed by High-Throughput Sequencing After Oral Doxycycline Administration in Beef Cattle.* Frontiers in Veterinary Science, 2020. **7**.
13. Henderson, G., et al., *Rumen microbial community composition varies with diet and host, but a core microbiome is found across a wide geographical range.* Scientific Reports, 2015. **5**(1): p. 14567.
14. Newbold, C.J. and E. Ramos-Morales, *Review: Ruminal microbiome and microbial metabolome: effects of diet and ruminant host.* Animal, 2020. **14**: p. s78-s86.
15. Diao, Q., R. Zhang, and T. Fu, *Review of Strategies to Promote Rumen Development in Calves.* Animals (Basel), 2019. **9**(8).
16. Jami, E., et al., *Exploring the bovine rumen bacterial community from birth to adulthood.* The ISME Journal, 2013. **7**(6): p. 1069-1079.
17. Amin, N. and J. Seifert, *Dynamic progression of the calf's microbiome and its influence on host health.* Computational and structural biotechnology journal, 2021. **19**: p. 989-1001.
18. Kelly, W.J., et al., *Genomic analysis of three Bifidobacterium species isolated from the calf gastrointestinal tract.* Scientific Reports, 2016. **6**(1): p. 30768.
19. Uyeno, Y., S. Shigemori, and T. Shimosato, *Effect of Probiotics/Prebiotics on Cattle Health and Productivity.* Microbes and environments, 2015. **30**(2): p. 126-132.

20. Huws, S.A., et al., *Addressing Global Ruminant Agricultural Challenges Through Understanding the Rumen Microbiome: Past, Present, and Future.* Frontiers in Microbiology, 2018. **9**(2161).
21. Grondin, J.M., et al., *Polysaccharide Utilization Loci: Fueling Microbial Communities.* J Bacteriol, 2017. **199**(15).
22. Flint, H.J., et al., *Links between diet, gut microbiota composition and gut metabolism.* Proceedings of the Nutrition Society, 2015. **74**(1): p. 13-22.
23. Sheridan, P.O., et al., *Polysaccharide utilization loci and nutritional specialization in a dominant group of butyrate-producing human colonic Firmicutes.* Microb Genom, 2016. **2**(2): p. e000043.
24. Briggs, J.A., J.M. Grondin, and H. Brumer, *Communal living: glycan utilization by the human gut microbiota.* Environmental Microbiology, 2021. **23**(1): p. 15-35.
25. Hess, M., et al., *Metagenomic Discovery of Biomass-Degrading Genes and Genomes from Cow Rumen.* Science, 2011. **331**(6016): p. 463.
26. Moraïs, S. and I. Mizrahi, *The Road Not Taken: The Rumen Microbiome, Functional Groups, and Community States.* Trends Microbiol, 2019. **27**(6): p. 538-549.
27. Tailford, L.E., et al., *Mucin glycan foraging in the human gut microbiome.* Frontiers in Genetics, 2015. **6**.
28. de Jesus Raposo, M.F., A.M.B. de Morais, and R.M.S.C. de Morais, *Marine polysaccharides from algae with potential biomedical applications.* Marine drugs, 2015. **13**(5): p. 2967-3028.
29. Fry, S.C., *Plant cell walls. From chemistry to biology.* Annals of Botany, 2011. **108**(1): p. viii-ix.
30. Kaur, N. and A.K. Gupta, *Applications of inulin and oligofructose in health and nutrition.* Journal of Biosciences, 2002. **27**(7): p. 703-714.
31. Vijn, I. and S. Smeekens, *Fructan: More Than a Reserve Carbohydrate?1.* Plant Physiology, 1999. **120**(2): p. 351-360.
32. Ritsema, T. and S. Smeekens, *Fructans: beneficial for plants and humans.* Curr Opin Plant Biol, 2003. **6**(3): p. 223-30.
33. Harrison, S., et al., *Linear Ion Trap MSn of Enzymatically Synthesized 13C-Labeled Fructans Revealing Differentiating Fragmentation Patterns of β (1-2) and β (1-6) Fructans and Providing a Tool for Oligosaccharide Identification in Complex Mixtures.* Analytical Chemistry, 2012. **84**(3): p. 1540-1548.
34. Van den Ende, W., *Multifunctional fructans and raffinose family oligosaccharides.* Frontiers in Plant Science, 2013. **4**(247).
35. Veenstra, L.D., J.-L. Jannink, and M.E. Sorrells, *Wheat Fructans: A Potential Breeding Target for Nutritionally Improved, Climate-Resilient Varieties.* Crop Science, 2017. **57**(3): p. 1624-1640.
36. Wei, J.-Z., et al., *Characterization of fructan biosynthesis in big bluegrass (Poa secunda).* Journal of Plant Physiology, 2002. **159**(7): p. 705-715.
37. Carpita, N.C., J. Kanabus, and T.L. Housley, *Linkage Structure of Fructans and Fructan Oligomers from Triticum aestivum and Festuca arundinacea Leaves.* Journal of Plant Physiology, 1989. **134**(2): p. 162-168.
38. Verspreet, J., et al., *Analysis of Storage and Structural Carbohydrates in Developing Wheat (Triticum aestivum L.) Grains Using Quantitative Analysis and*

Microscopy. Journal of Agricultural and Food Chemistry, 2013. **61**(38): p. 9251-9259.
39. Verspreet, J., et al., *Cereal grain fructans: Structure, variability and potential health effects.* Trends in Food Science & Technology, 2015. **43**(1): p. 32-42.
40. Shiomi, N., *Properties of Fructosyltransferases Involved in the Synthesis of Fructan in Liliaceous Plants.* Journal of Plant Physiology, 1989. **134**(2): p. 151-155.
41. Hendry, G.A.F., *Evolutionary origins and natural functions of fructans – a climatological, biogeographic and mechanistic appraisal.* New Phytologist, 1993. **123**(1): p. 3-14.
42. Joudi, M., et al., *Comparison of fructan dynamics in two wheat cultivars with different capacities of accumulation and remobilization under drought stress.* Physiologia Plantarum, 2012. **144**(1): p. 1-12.
43. Pilon-Smits, E.A.H., et al., *Improved Performance of Transgenic Fructan-Accumulating Tobacco under Drought Stress.* Plant Physiology, 1995. **107**(1): p. 125-130.
44. Kafi, M., W.S. Stewart, and A.M. Borland, *Carbohydrate and Proline Contents in Leaves, Roots, and Apices of Salt-Tolerant and Salt-Sensitive Wheat Cultivars1.* Russian Journal of Plant Physiology, 2003. **50**(2): p. 155-162.
45. Livingston, D.P., 3rd, D.K. Hincha, and A.G. Heyer, *Fructan and its relationship to abiotic stress tolerance in plants.* Cell Mol Life Sci, 2009. **66**(13): p. 2007-23.
46. Komor, E., *Source physiology and assimilate transport: the interaction of sucrose metabolism, starch storage and phloem export in source leaves and the effects on sugar status in phloem.* Australian Journal of Plant Physiology, 2000. **27**: p. 497-505.
47. Huynh, B.-L., et al., *Genotypic variation in wheat grain fructan content revealed by a simplified HPLC method.* Journal of Cereal Science, 2008. **48**(2): p. 369-378.
48. Nemeth, C., et al., *Relationship of Grain Fructan Content to Degree of Polymerisation in Different Barleys.* Food and Nutrition Sciences, 2014. **05**: p. 581-589.
49. Nardi, S., et al., *Nutritional benefits of developing cereals for functional foods.* Cereal Research Communications, 2003. **31**(3/4): p. 445-452.
50. Nilsson, U., A. Dahlqvist, and B. Nilsson, *Cereal fructosans: Part 2—Characterization and structure of wheat fructosans.* Food Chemistry, 1986. **22**(2): p. 95-106.
51. Ominski, K., et al., *Utilization of by-products and food waste in livestock production systems: a Canadian perspective.* Animal Frontiers, 2021. **11**(2): p. 55-63.
52. Carlsson, R., *Food and Non-Food Uses of Immature Cereals*, in *Cereals: Novel Uses and Processes*, G.M. Campbell, C. Webb, and S.L. McKee, Editors. 1997, Springer US: Boston, MA. p. 159-167.
53. Lombard, V., et al., *The carbohydrate-active enzymes database (CAZy) in 2013.* Nucleic Acids Res, 2014. **42**(Database issue): p. D490-5.
54. CAZY, C.A.e.D.
55. Drula, E., et al., *The carbohydrate-active enzyme database: functions and literature.* Nucleic acids research, 2022. **50**(D1): p. D571-D577.

56. Jones, D.R., et al., *SACCHARIS: an automated pipeline to streamline discovery of carbohydrate active enzyme activities within polyspecific families and de novo sequence datasets.* Biotechnology for Biofuels, 2018. **11**(1): p. 27.
57. Zhang, H., et al., *dbCAN2: a meta server for automated carbohydrate-active enzyme annotation.* Nucleic acids research, 2018. **46**(W1): p. W95-W101.
58. Yin, Y., et al., *dbCAN: a web resource for automated carbohydrate-active enzyme annotation.* Nucleic Acids Research, 2012. **40**(W1): p. W445-W451.
59. Barrett, K., et al., *Conserved unique peptide patterns (CUPP) online platform: peptide-based functional annotation of carbohydrate active enzymes.* Nucleic Acids Research, 2020. **48**(W1): p. W110-W115.
60. Xu, J., et al., *eCAMI: simultaneous classification and motif identification for enzyme annotation.* Bioinformatics, 2019. **36**(7): p. 2068-2075.
61. Cimini, S., et al., *GH32 family activity: a topological approach through protein contact networks.* Plant Molecular Biology, 2016. **92**(4): p. 401-410.
62. Lammens, W., et al., *Structural insights into glycoside hydrolase family 32 and 68 enzymes: functional implications.* Journal of Experimental Botany, 2009. **60**(3): p. 727-740.
63. Gibson, G.R., et al., *Expert consensus document: The International Scientific Association for Probiotics and Prebiotics (ISAPP) consensus statement on the definition and scope of prebiotics.* Nature reviews Gastroenterology & hepatology, 2017. **14**(8): p. 491.
64. Hill, C., et al., *The International Scientific Association for Probiotics and Prebiotics consensus statement on the scope and appropriate use of the term probiotic.* Nature Reviews Gastroenterology & Hepatology, 2014. **11**(8): p. 506-514.
65. Scott, K.P., et al., *Developments in understanding and applying prebiotics in research and practice—an ISAPP conference paper.* Journal of Applied Microbiology, 2020. **128**(4): p. 934-949.
66. Gaggìa, F., P. Mattarelli, and B. Biavati, *Probiotics and prebiotics in animal feeding for safe food production.* International Journal of Food Microbiology, 2010. **141**: p. S15-S28.
67. Markowiak, P. and K. Śliżewska, *The role of probiotics, prebiotics and synbiotics in animal nutrition.* Gut Pathogens, 2018. **10**(1): p. 21.
68. Grand, E., et al., *Effects of short-chain fructooligosaccharides on growth performance of preruminant veal calves.* Journal of Dairy Science, 2013. **96**(2): p. 1094-1101.
69. Pineda, A., et al., *Evaluation of serum protein-based arrival formula and serum protein supplement (Gammulin) on growth, morbidity, and mortality of stressed (transport and cold) male dairy calves.* Journal of Dairy Science, 2016. **99**(11): p. 9027-9039.
70. Hill, T.M., et al., *Oligosaccharides for Dairy Calves.* The Professional Animal Scientist, 2008. **24**(5): p. 460-464.
71. Quigley, J.D., 3rd, C.J. Kost, and T.A. Wolfe, *Effects of spray-dried animal plasma in milk replacers or additives containing serum and oligosaccharides on growth and health of calves.* J Dairy Sci, 2002. **85**(2): p. 413-21.
72. Tian, K., et al., *Effects of dietary supplementation of inulin on rumen fermentation and bacterial microbiota, inflammatory response and growth performance in*

finishing beef steers fed high or low-concentrate diet. Animal Feed Science and Technology, 2019. **258**: p. 114299.
73. Casiraghi, M.C., et al., *Prebiotic potential and gastrointestinal effects of immature wheat grain (IWG) biscuits.* Antonie van Leeuwenhoek, 2011. **99**(4): p. 795-805.
74. Merendino, N., et al., *Chemical characterization and biological effects of immature durum wheat in rats.* Journal of Cereal Science, 2006. **43**(2): p. 129-136.
75. Thomas, F., et al., *Environmental and Gut Bacteroidetes: The Food Connection.* Frontiers in Microbiology, 2011. **2**(93).
76. Nocek, J.E. and W.P. Kautz, *Direct-fed microbial supplementation on ruminal digestion, health, and performance of pre- and postpartum dairy cattle.* J Dairy Sci, 2006. **89**(1): p. 260-6.
77. Nocek, J.E., et al., *Ruminal supplementation of direct-fed microbials on diurnal pH variation and in situ digestion in dairy cattle.* J Dairy Sci, 2002. **85**(2): p. 429-33.
78. Cangiano, L.R., et al., *Invited Review: Strategic use of microbial-based probiotics and prebiotics in dairy calf rearing.* Applied Animal Science, 2020. **36**(5): p. 630-651.
79. Swanson, K.S., et al., *The International Scientific Association for Probiotics and Prebiotics (ISAPP) consensus statement on the definition and scope of synbiotics.* Nature Reviews Gastroenterology & Hepatology, 2020. **17**(11): p. 687-701.
80. Gibson, G.R., et al., *Selective stimulation of bifidobacteria in the human colon by oligofructose and inulin.* Gastroenterology, 1995. **108**(4): p. 975-82.
81. Peshev, D. and W. Van den Ende, *Fructans: Prebiotics and immunomodulators.* Journal of Functional Foods, 2014. **8**: p. 348-357.
82. Glabe, C.G., P.K. Harty, and S.D. Rosen, *Preparation and properties of fluorescent polysaccharides.* Anal Biochem, 1983. **130**(2): p. 287-94.
83. Arnosti, C., *Measurement of depth- and site-related differences in polysaccharide hydrolysis rates in marine sediments.* Geochimica et Cosmochimica Acta, 1995. **59**(20): p. 4247-4257.
84. Reintjes, G., et al., *An alternative polysaccharide uptake mechanism of marine bacteria.* The ISME Journal, 2017. **11**(7): p. 1640-1650.
85. Hehemann, J.-H., et al., *Single cell fluorescence imaging of glycan uptake by intestinal bacteria.* The ISME Journal, 2019. **13**(7): p. 1883-1889.
86. Klassen, L., et al., *Quantifying fluorescent glycan uptake to elucidate strain-level variability in foraging behaviors of rumen bacteria.* Microbiome, 2021. **9**(1): p. 23.
87. Kozłowska, I., J. Marć-Pieńkowska, and M. Bednarczyk, *2. Beneficial Aspects of Inulin Supplementation as a Fructooligosaccharide Prebiotic in Monogastric Animal Nutrition – A Review.* Annals of Animal Science, 2016. **16**(2): p. 315-331.
88. Kolida, S., K. Tuohy, and G.R. Gibson, *Prebiotic effects of inulin and oligofructose.* Br J Nutr, 2002. **87 Suppl 2**: p. S193-7.
89. Hidaka, H., Y. Tashiro, and T. Eida, *Proliferation of Bifidobacteria by Oligosaccharides and Their Useful Effect on Human Health.* Bifidobacteria and Microflora, 1991. **10**: p. 65-79.
90. Reis, S., et al., *Mechanisms used by inulin-type fructans to improve the lipid profile.* Nutricion hospitalaria, 2014. **31**: p. 528-534.

91. Vogt, L., et al., *Immunological Properties of Inulin-Type Fructans.* Critical Reviews in Food Science and Nutrition, 2015. **55**(3): p. 414-436.
92. Tsai, C.C., et al., *The immunologically active oligosaccharides isolated from wheatgrass modulate monocytes via Toll-like receptor-2 signaling.* J Biol Chem, 2013. **288**(24): p. 17689-97.
93. Xu, Q., et al., *Levan (β-2, 6-fructan), a major fraction of fermented soybean mucilage, displays immunostimulating properties via Toll-like receptor 4 signalling: induction of interleukin-12 production and suppression of T-helper type 2 response and immunoglobulin E production.* Clinical & Experimental Allergy, 2006. **36**(1): p. 94-101.
94. Gomez, E., et al., *In vitro evaluation of the fermentation properties and potential prebiotic activity of Agave fructans.* J Appl Microbiol, 2010. **108**(6): p. 2114-21.
95. Tarini, J. and T.M. Wolever, *The fermentable fibre inulin increases postprandial serum short-chain fatty acids and reduces free-fatty acids and ghrelin in healthy subjects.* Appl Physiol Nutr Metab, 2010. **35**(1): p. 9-16.
96. Van den Abbeele, P., et al., *Fructans with Varying Degree of Polymerization Enhance the Selective Growth of Bifidobacterium animalis subsp. lactis BB-12 in the Human Gut Microbiome In Vitro.* Applied Sciences, 2021. **11**(2): p. 598.
97. Mueller, M., et al., *Growth of selected probiotic strains with fructans from different sources relating to degree of polymerization and structure.* Journal of Functional Foods, 2016. **24**: p. 264-275.
98. Keith, J., et al., *The Production, Purification and Properties of the Biopolymer Levan Produced by the Bacterium Erwinia Herbicola.* 1989.
99. Silbir, S., et al., *Levan production by Zymomonas mobilis in batch and continuous fermentation systems.* Carbohydr Polym, 2014. **99**: p. 454-61.
100. Chatterton, N.J., et al., *Carbohydrate Partitioning in 185 Accessions of Gramineae Grown Under Warm and Cool Temperatures.* Journal of Plant Physiology, 1989. **134**(2): p. 169-179.
101. LIVINGSTON III, D.P., N.J. CHATTERTON, and P.A. HARRISON, *Structure and quantity of fructan oligomers in oat (Avena spp.).* New Phytologist, 1993. **123**(4): p. 725-734.
102. Verspreet, J., et al., *LC-MS analysis reveals the presence of graminan- and neo-type fructans in wheat grains.* Journal of Cereal Science, 2015. **61**: p. 133-138.
103. Karppinen, S., et al., *Fructan Content of Rye and Rye Products.* Cereal Chemistry, 2003. **80**(2): p. 168-171.
104. Livingston, D.P., D.K. Hincha, and A.G. Heyer, *Fructan and its relationship to abiotic stress tolerance in plants.* Cellular and Molecular Life Sciences, 2009. **66**(13): p. 2007-2023.
105. Scofield, G.N., et al., *Starch storage in the stems of wheat plants: localization and temporal changes.* Annals of Botany, 2009. **103**(6): p. 859-868.
106. Cairns, A.J., et al., *Fructan Biosynthesis in Excised Leaves of Lolium temulentum. VII. Sucrose and Fructan Hydrolysis by a Fructan-Polymerizing Enzyme Preparation.* The New Phytologist, 1997. **136**(1): p. 61-72.
107. Franco-Robles, E. and M.G. López, *Implication of fructans in health: immunomodulatory and antioxidant mechanisms.* TheScientificWorldJournal, 2015. **2015**: p. 289267-289267.

108. Astó, E., et al., *Effect of the Degree of Polymerization of Fructans on Ex Vivo Fermented Human Gut Microbiome.* Nutrients, 2019. **11**(6): p. 1293.
109. Paßlack, N., W. Vahjen, and J. Zentek, *Dietary inulin affects the intestinal microbiota in sows and their suckling piglets.* BMC veterinary research, 2015. **11**: p. 51-51.
110. Xia, Y., et al., *Effects of dietary inulin supplementation on the composition and dynamics of cecal microbiota and growth-related parameters in broiler chickens.* Poultry Science, 2019. **98**(12): p. 6942-6953.
111. Scardovi, V., et al., *Bifidobacterium cuniculi, Bifidobacterium choerinum, Bifidobacterium boum, and Bifidobacterium pseudocatenulatum.* International Journal of Systematic and Evolutionary Microbiology, 1979. **29**(4): p. 291-311.
112. Biavati, B. and P. Mattarelli, *Bifidobacterium ruminantium sp. nov. and Bifidobacterium merycicum sp. nov. from the rumens of cattle.* Int J Syst Bacteriol, 1991. **41**(1): p. 163-8.
113. BIAVATI, B., V. SCARDOVI, and W.E.C. MOORE, *Electrophoretic Patterns of Proteins in the Genus Bifidobacterium and Proposal of Four New Species.* International Journal of Systematic and Evolutionary Microbiology, 1982. **32**(3): p. 358-373.
114. Sharpe, M.E., et al., *Two New Species of Lactobacillus Isolated from the Bovine Rumen, Lactobacillus ruminis sp.nov. and Lactobacillus vitulinus sp.nov.* Microbiology, 1973. **77**(1): p. 37-49.
115. Yin, Y., et al., *dbCAN: a web resource for automated carbohydrate-active enzyme annotation.* Nucleic Acids Res, 2012. **40**(Web Server issue): p. W445-51.
116. McCleary, B., et al., *Measurement of Total Fructan in Foods by Enzymatic/Spectrophotometric Method: Collaborative Study.* Journal of AOAC International, 2000. **83**: p. 356-364.
117. Verspreet, J., et al., *A new high-throughput LC-MS method for the analysis of complex fructan mixtures.* Analytical and Bioanalytical Chemistry, 2014. **406**(19): p. 4785-4788.
118. Jones, P., et al., *InterProScan 5: genome-scale protein function classification.* Bioinformatics, 2014. **30**(9): p. 1236-1240.
119. Edgar, R.C., *MUSCLE: a multiple sequence alignment method with reduced time and space complexity.* BMC Bioinformatics, 2004. **5**(1): p. 113.
120. Nardi, S., et al., *Nutritional benefits of developing cereals for functional foods.* Cereal Research Communications, 2003. **31**(3): p. 445-452.
121. Huynh, B.L., et al., *Quantitative trait loci for grain fructan concentration in wheat (Triticum aestivum L.).* Theor Appl Genet, 2008. **117**(5): p. 701-9.
122. Ruuska, S., et al., *Genotypic variation in water-soluble carbohydrate accumulation in wheat.* Functional Plant Biology - FUNCT PLANT BIOL, 2006. **33**.
123. Arnosti, C., *Fluorescent derivatization of polysaccharides and carbohydrate-containing biopolymers for measurement of enzyme activities in complex media.* Journal of Chromatography B, 2003. **793**(1): p. 181-191.
124. Zeng, L., Z.T. Wen, and R.A. Burne, *A novel signal transduction system and feedback loop regulate fructan hydrolase gene expression in Streptococcus mutans.* Molecular Microbiology, 2006. **62**(1): p. 187-200.

125. Burne, R.A., et al., *Expression, purification, and characterization of an exo-beta-D-fructosidase of Streptococcus mutans.* J Bacteriol, 1987. **169**(10): p. 4507-17.
126. Cuskin, F., et al., *How nature can exploit nonspecific catalytic and carbohydrate binding modules to create enzymatic specificity.* Proc Natl Acad Sci U S A, 2012. **109**(51): p. 20889-94.
127. Devika, N.T. and K. Raman, *Deciphering the metabolic capabilities of Bifidobacteria using genome-scale metabolic models.* Scientific Reports, 2019. **9**(1): p. 18222.
128. BIAVATI, B. and P. MATTARELLI, *Bifidobacterium ruminantium sp. nov. and Bifidobacterium merycicum sp. nov. from the Rumens of Cattle.* International Journal of Systematic and Evolutionary Microbiology, 1991. **41**(1): p. 163-168.
129. Jenkins, C.L.D., et al., *Chain length of cereal fructans isolated from wheat stem and barley grain modulates in vitro fermentation.* Journal of Cereal Science, 2011. **53**(2): p. 188-191.
130. Verspreet, J., et al., *Maximizing the Concentrations of Wheat Grain Fructans in Bread by Exploring Strategies To Prevent Their Yeast (Saccharomyces cerevisiae)-Mediated Degradation.* Journal of Agricultural and Food Chemistry, 2013. **61**(6): p. 1397-1404.
131. Nilsson, U., R. Öste, and M. Jägerstad, *Cereal fructans: Hydrolysis by yeast invertase, in vitro and during fermentation.* Journal of Cereal Science, 1987. **6**(1): p. 53-60.
132. Böhm, A., et al., *Heat-induced degradation of inulin.* European Food Research and Technology, 2005. **220**(5): p. 466-471.
133. Man, J.C.d., M. Rogosa, and M.E. Sharpe, *A MEDIUM FOR THE CULTIVATION OF LACTOBACILLI.* Journal of Applied Microbiology, 1960. **23**: p. 130-135.
134. Darriba, D., et al., *ProtTest 3: fast selection of best-fit models of protein evolution.* Bioinformatics, 2011. **27**(8): p. 1164-5.
135. Price, M.N., P.S. Dehal, and A.P. Arkin, *FastTree: Computing Large Minimum Evolution Trees with Profiles instead of a Distance Matrix.* Molecular Biology and Evolution, 2009. **26**(7): p. 1641-1650.
136. Wickham, H., *ggplot2: Elegant Graphics for Data Analysis.* 2016: Springer-Verlag New York.
137. Yu, G., et al., *ggtree: an r package for visualization and annotation of phylogenetic trees with their covariates and other associated data.* Methods in Ecology and Evolution, 2017. **8**(1): p. 28-36.
138. Wickham, H., *The Split-Apply-Combine Strategy for Data Analysis.* Journal of Statistical Software, 2011. **40**(1): p. 1 - 29.
139. Wang, L.G., et al., *Treeio: An R Package for Phylogenetic Tree Input and Output with Richly Annotated and Associated Data.* Mol Biol Evol, 2020. **37**(2): p. 599-603.
140. Lassey, K., *Livestock methane emission and its perspective in the global methane cycle.* Australian Journal of Experimental Agriculture - AUST J EXP AGR, 2008. **48**.
141. Steinfeld, H. and T. Wassenaar, *The Role of Livestock Production in Carbon and Nitrogen Cycles.* Annual Review of Environment and Resources, 2007. **32**(1): p. 271-294.

142. Legesse, G., et al., *Greenhouse gas emissions of Canadian beef production in 1981 as compared with 2011.* Animal Production Science, 2016. **56**(3): p. 153-168.
143. Simon, P.L., et al., *Nitrous oxide emission factors from cattle urine and dung, and dicyandiamide (DCD) as a mitigation strategy in subtropical pastures.* Agriculture, Ecosystems & Environment, 2018. **267**: p. 74-82.
144. Pogue, S.J., et al., *A social-ecological systems approach for the assessment of ecosystem services from beef production in the Canadian prairie.* Ecosystem Services, 2020. **45**: p. 101172.
145. Watkinson, A. and S. Ormerod, *Grasslands, grazing and biodiversity: Editors' introduction.* Journal of Applied Ecology, 2001. **38**: p. 233-237.
146. Mottet, A., et al., *Livestock: On our plates or eating at our table? A new analysis of the feed/food debate.* Global Food Security, 2017. **14**: p. 1-8.
147. Hernandez-Sanabria, E., et al., *Influence of Sire Breed on the Interplay among Rumen Microbial Populations Inhabiting the Rumen Liquid of the Progeny in Beef Cattle.* PLOS ONE, 2013. **8**(3): p. e58461.
148. Benson, A.K., et al., *Individuality in gut microbiota composition is a complex polygenic trait shaped by multiple environmental and host genetic factors.* Proceedings of the National Academy of Sciences, 2010. **107**(44): p. 18933-18938.
149. Schelling, G.T., *Monensin mode of action in the rumen.* J Anim Sci, 1984. **58**(6): p. 1518-27.
150. Beharka, A.A., T.G. Nagaraja, and J.L. Morrill, *Performance and ruminal function development of young calves fed diets with Aspergillus oryzae fermentation extract.* J Dairy Sci, 1991. **74**(12): p. 4326-36.
151. Lesmeister, K.E., A.J. Heinrichs, and M.T. Gabler, *Effects of supplemental yeast (Saccharomyces cerevisiae) culture on rumen development, growth characteristics, and blood parameters in neonatal dairy calves.* J Dairy Sci, 2004. **87**(6): p. 1832-9.
152. Beauchemin, K.A. and S.M. McGinn, *Methane emissions from beef cattle: effects of fumaric acid, essential oil, and canola oil.* J Anim Sci, 2006. **84**(6): p. 1489-96.
153. Macheboeuf, D., et al., *Dose–response effects of essential oils on in vitro fermentation activity of the rumen microbial population.* Animal Feed Science and Technology, 2008. **145**(1): p. 335-350.
154. Zhang, J., et al., *Effect of Dietary Forage to Concentrate Ratios on Dynamic Profile Changes and Interactions of Ruminal Microbiota and Metabolites in Holstein Heifers.* Frontiers in Microbiology, 2017. **8**.
155. Wang, L., et al., *The Effects of Different Concentrate-to-Forage Ratio Diets on Rumen Bacterial Microbiota and the Structures of Holstein Cows During the Feeding Cycle.* Animals : an open access journal from MDPI, 2020. **10**(6): p. 957.
156. Chen, H., et al., *Effects of dietary forage to concentrate ratio on nutrient digestibility, ruminal fermentation and rumen bacterial composition in Angus cows.* Scientific Reports, 2021. **11**(1): p. 17023.
157. Wallace, R.J. and C.J. Newbold. *Rumen fermentation and its manipulation: the development of yeast cultures as feed additives*. 1993.

158. Myer, P.R., et al., *Analysis of the gut bacterial communities in beef cattle and their association with feed intake, growth, and efficiency.* J Anim Sci, 2017. **95**(7): p. 3215-3224.
159. Smith, P.E., et al., *Differences in the Composition of the Rumen Microbiota of Finishing Beef Cattle Divergently Ranked for Residual Methane Emissions.* Frontiers in Microbiology, 2022. **13**.
160. Khafipour, E., et al., *Rumen Microbiome Composition Determined Using Two Nutritional Models of Subacute Ruminal Acidosis.* Applied and Environmental Microbiology, 2009. **75**(22): p. 7115-7124.
161. Wang, X., et al., *Correlation between composition of the bacterial community and concentration of volatile fatty acids in the rumen during the transition period and ketosis in dairy cows.* Applied and environmental microbiology, 2012. **78**(7): p. 2386-2392.
162. Meyer, D. and M. Stasse-Wolthuis, *The bifidogenic effect of inulin and oligofructose and its consequences for gut health.* European Journal of Clinical Nutrition, 2009. **63**(11): p. 1277-1289.
163. Xia, B., et al., *Gut microbiota mediates the effects of inulin on enhancing sulfomucin production and mucosal barrier function in a pig model.* Food & Function, 2021. **12**(21): p. 10967-10982.
164. Guo, Y., et al., *Inulin supplementation ameliorates hyperuricemia and modulates gut microbiota in Uox-knockout mice.* European Journal of Nutrition, 2021. **60**: p. 1-14.
165. Wang, Y., et al., *Dietary supplementation with inulin improves lactation performance and serum lipids by regulating the rumen microbiome and metabolome in dairy cows.* Animal nutrition (Zhongguo xu mu shou yi xue hui), 2021. **7**(4): p. 1189-1204.
166. Zhao, Y., et al., *Responses of Lactation, Rumen Fermentation and Blood Biochemical Parameters with Increasing Dietary Inulin Supplementation in Mid-Lactation Dairy Cows.* Agriculture, 2022. **12**(4): p. 521.
167. Marteau, P., et al., *Comparative Study of Bacterial Groups within the Human Cecal and Fecal Microbiota.* Applied and Environmental Microbiology, 2001. **67**(10): p. 4939-4942.
168. Sghir, A., D. Antonopoulos, and R.I. Mackie, *Design and Evaluation of a Lactobacillus Group-specific Ribosomal RNA-targeted Hybridization Probe and its Application to the Study of Intestinal Microecology in Pigs.* Systematic and Applied Microbiology, 1998. **21**(2): p. 291-296.
169. Bergman, E.N., *Energy contributions of volatile fatty acids from the gastrointestinal tract in various species.* Physiol Rev, 1990. **70**(2): p. 567-90.
170. Penner, G.B., et al., *RUMINANT NUTRITION SYMPOSIUM: Molecular adaptation of ruminal epithelia to highly fermentable diets1.* Journal of Animal Science, 2011. **89**(4): p. 1108-1119.
171. Górka, P., et al., *Invited review: Use of butyrate to promote gastrointestinal tract development in calves.* Journal of Dairy Science, 2018. **101**(6): p. 4785-4800.
172. Wiltrout, D.W. and L.D. Satter, *Contribution of propionate to glucose synthesis in the lactating and nonlactating cow.* J Dairy Sci, 1972. **55**(3): p. 307-17.
173. Umucalilar, D., et al., *Potential role of inulin in rumen fermentation.* Revue de médecine vétérinaire, 2010. **161**: p. 3-9.

174. Poulsen, M., B.B. Jensen, and R.M. Engberg, *The effect of pectin, corn and wheat starch, inulin and pH on in vitro production of methane, short chain fatty acids and on the microbial community composition in rumen fluid.* Anaerobe, 2012. **18**(1): p. 83-90.
175. Firkins, J.L. and Z. Yu, *RUMINANT NUTRITION SYMPOSIUM: How to use data on the rumen microbiome to improve our understanding of ruminant nutrition.* J Anim Sci, 2015. **93**(4): p. 1450-70.
176. Suzuki, M., *Fructans in Forage Grasses with Varying Degrees of Coldhardiness.* Journal of Plant Physiology, 1989. **134**(2): p. 224-231.
177. Klassen, L., et al., *Yeast-based prebiotic and Bacteroides probiotics affect rumen microbiome composition and fermentation.* 2022.
178. Cuskin, F., et al., *Human gut Bacteroidetes can utilize yeast mannan through a selfish mechanism.* Nature, 2015. **517**(7533): p. 165-169.
179. Rada, V., et al., *Enrichment of bifidobacteria in the hen caeca by dietary inulin.* Folia Microbiol (Praha), 2001. **46**(1): p. 73-5.
180. Shang, H.M., et al., *Effects of inulin on performance, egg quality, gut microflora and serum and yolk cholesterol in laying hens.* British Poultry Science, 2010. **51**(6): p. 791-796.
181. van Zyl, W.F., S.M. Deane, and L.M.T. Dicks, *Molecular insights into probiotic mechanisms of action employed against intestinal pathogenic bacteria.* Gut Microbes, 2020. **12**(1): p. 1831339.
182. Fukuda, S., et al., *Bifidobacteria can protect from enteropathogenic infection through production of acetate.* Nature, 2011. **469**(7331): p. 543-7.
183. Glatter, M., et al., *Modification of the equine gastrointestinal microbiota by Jerusalem artichoke meal supplementation.* PLOS ONE, 2019. **14**(8): p. e0220553.
184. Bucław, M., *The use of inulin in poultry feeding: A review.* Journal of Animal Physiology and Animal Nutrition, 2016. **100**.
185. Loh, G., et al., *Inulin alters the intestinal microbiota and short-chain fatty acid concentrations in growing pigs regardless of their basal diet.* J Nutr, 2006. **136**(5): p. 1198-202.
186. Qiu, Q., et al., *Temporal Dynamics in Rumen Bacterial Community Composition of Finishing Steers during an Adaptation Period of Three Months.* Microorganisms, 2019. **7**(10): p. 410.
187. Bushnell, B., J. Rood, and E. Singer, *BBMerge - Accurate paired shotgun read merging via overlap.* PloS one, 2017. **12**(10): p. e0185056-e0185056.
188. Quast, C., et al., *The SILVA ribosomal RNA gene database project: improved data processing and web-based tools.* Nucleic acids research, 2013. **41**(Database issue): p. D590-D596.
189. McMurdie, P.J. and S. Holmes, *phyloseq: An R Package for Reproducible Interactive Analysis and Graphics of Microbiome Census Data.* PLOS ONE, 2013. **8**(4): p. e61217.
190. Kembel, S.W., et al., *Picante: R tools for integrating phylogenies and ecology.* Bioinformatics, 2010. **26**(11): p. 1463-1464.
191. Juggins, S., *rioja: Analysis of Quaternary Science Data*. 2020.
192. Wallace, R.J., et al., *A heritable subset of the core rumen microbiome dictates dairy cow productivity and emissions.* Sci Adv, 2019. **5**(7): p. eaav8391.

193. Mizrahi, I., R.J. Wallace, and S. Moraïs, *The rumen microbiome: balancing food security and environmental impacts.* Nature Reviews Microbiology, 2021. **19**(9): p. 553-566.
194. Playne, M.J., *Determination of ethanol, volatile fatty acids, lactic and succinic acids in fermentation liquids by gas chromatography.* Journal of the Science of Food and Agriculture, 1985. **36**(8): p. 638-644.
195. Cottyn, B.G. and C.V. Boucque, *Rapid method for the gas-chromatographic determination of volatile fatty acids in rumen fluid.* Journal of Agricultural and Food Chemistry, 1968. **16**(1): p. 105-107.
196. Bennke, C.M., et al., *Modification of a High-Throughput Automatic Microbial Cell Enumeration System for Shipboard Analyses.* Applied and Environmental Microbiology, 2016. **82**(11): p. 3289-3296.
197. Olfert, E.D., C.B. M., and A.A. McWilliam, *Guide to the Care and Use of Experimental Animals*. 2nd ed. Vol. 1. 1993, Ottawa, ON: C. C.o. A. Care.
198. Rhine, E.D., et al., *Improving the Berthelot Reaction for Determining Ammonium in Soil Extracts and Water.* Soil Science Society of America Journal, 1998. **62**(2): p. 473-480.
199. Gentry, C.E. and R.B. Willis, *Improved method for automated determination of ammonium in soil extracts.* Communications in Soil Science and Plant Analysis, 1988. **19**(6): p. 721-737.

Appendix 1

Supplementary table and figures

Supplemental Table 1: CAZome analysis of bovine-adapted *Bifidobacterium* and *Lactobacillus* species for the major glycoside hydrolase (GH) families involved in plant cell wall degradation.

CAZy family	Major known activity	L. ruminis (ATCC 27780)	L. vitulinus (ATCC 27783)	B. ruminantium (ATCC 49390)	B. merycicum (ATCC 49391)	B. boum (ATCC 27917)	B. globosum (ATCC 25865)
Cellulose- and pectin- active							
GH5	cellulase	0	0	1	1	1	0
GH8	endo-xylanases	0	0	0	1	0	0
	Total	0	0	1	2	1	0
Cell wall elongation							
GH16	xyloglucanases & xyloglycosyltransferases	0	0	0	1	0	0
	Total	0	0	0	1	0	0
Debranching enzymes							
GH51	α-L-arabinofuranosidase	0	0	0	0	1	1
GH67	α-glucuronidase	0	3	2	2	2	2
GH77	4-α-glucanotransferase	0	3	2	2	2	2
GH78	α-L-rhamnosidase	0	1	1	0	0	0
GH146	β-L-arabinofuranosidase	0	0	0	0	0	1
	Total	0	7	5	4	5	6
Oligosaccharide-degrading enzymes							
GH1	β-glucosidase and many other β-linked dimers	4	10	0	0	0	1
GH2	β-galactosidases and other β-linked dimers	0	0	2	1	0	3
GH3	mainly β-glucosidases	1	1	4	3	1	2
GH13	α-amylase	6	5	15	15	18	17
GH31	α-glucosidase	0	0	1	0	1	1
GH32	inulinase, levanase	1	5	1	2	1	1
GH42	β-galactosidase	0	0	1	2	1	1
GH43	arabinases & xylosidases	0	0	0	4	1	7
GH94	cellobiose phosphorylase	0	0	0	1	0	1
	Total	12	21	24	28	23	34

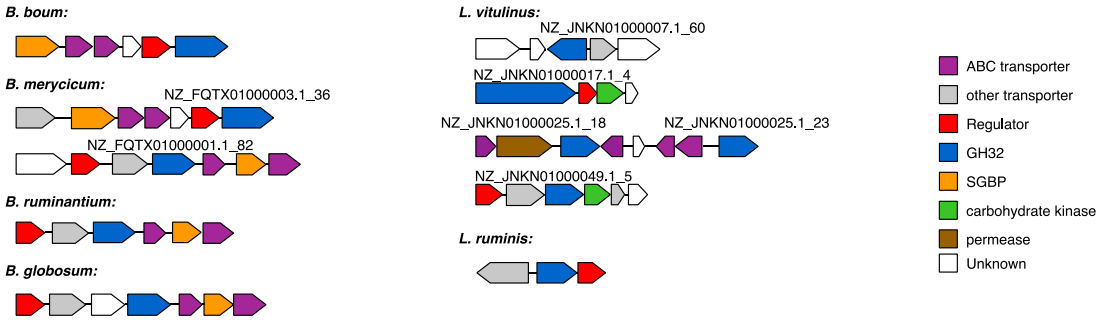

Supplemental Figure 1: Gene clusters for fructan metabolism in rumen-adapted *Bifidobacterium* and *Lactobacillus* species

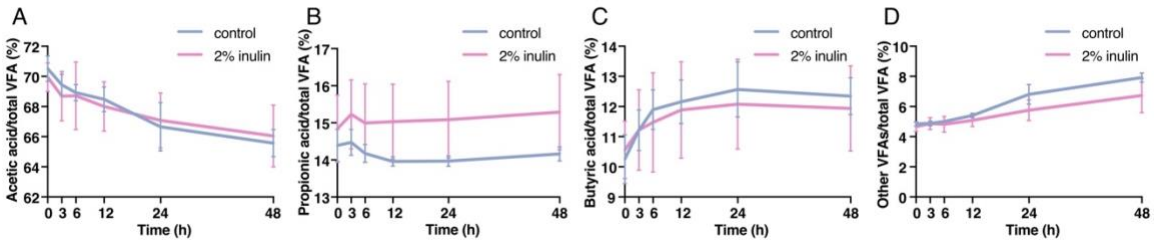

Supplementary Figure 2: Production of VFAs in artificial rumen systems seeded with inulin-adapted microbial communities. Cattle were fed a basal or 2% inulin supplemented diet for 17 d prior to sampling and *ex vivo* measurements were conducted, where **(A)** acetic acid, **(B)** propionic acid, **(C)** butyric acid, and **(D)** other VFAs are plotted as a percentage of the total.

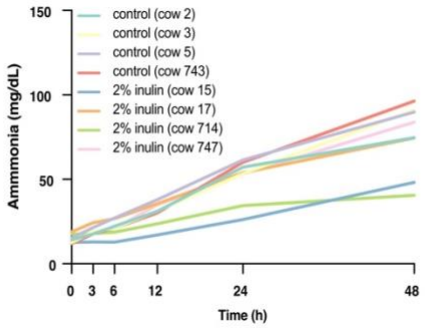

Supplementary Figure 3: Production of ammonia in artificial rumen systems seeded with inulin-adapted microbial communities. Cattle were fed diet a basal or 2% inulin supplemented diet for 17 d prior to sampling and *ex vivo* measurements were conducted, where individual cow ammonia production profiles are shown. Cow 15 (blue) and cow 714 (green) were fed a diet supplemented with 2% inulin showed a decreased production of ammonia.